EYE-CLIMA
Verifying emissions of climate forcers

High-resolution fluxes and uncertainties of CO_2, CH_4 and N_2O for Europe

DELIVERABLE 2.3

Author(s):	Tuula Aalto, Philippe Peylin, Almut Arneth, Jianyong Ma, Tiina Markkanen, Henri Sulkava, Vladislav Bastrikov, Elodie Salmon

Date of submission:	28-06-2024
Version:	1.0
Responsible partner:	FMI
Deliverable due date:	31-12-2023
Dissemination level:	Public

Call:	HORIZON-CL5-2022-D1-02
Topic:	Climate Sciences and Responses
Project Type:	Research and Innovation Action
Lead Beneficiary:	NILU - Norsk Institutt for Luftforskning

This project has received funding from the European Union's Horizon Europe research and innovation programme under grant agreement No 101081395

Document History

Version	Date	Comment	Modifications made by
0.1	05-02-2024	First Draft	Tuula Aalto, Philippe Peylin, Almut Arneth, Jianyong Ma, Tiina Markkanen, Henri Sulkava, Vladislav Bastrikov, Elodie Salmon
0.2	13-06-2024	Second draft sent to consortium	Philippe Peylin, Jianyong Ma, Tuula Aalto
0.3	17-06-2024	Internal review	Antoine Berchet
0.4	26-06-2024	Final draft sent to coordination team	Tuula Aalto
0.5	27-06-2024	Final draft formatted	Rona Thompson
1.0	28-06-2024	Submitted to Commission	Rona Thompson

This project has received funding from the European Union's Horizon Europe research and innovation programme under grant agreement No 101081395

Summary

The primary objective of this deliverable is to provide policy relevant estimates of major GHG fluxes: CO_2 (see Section 2), N_2O (see Section 3), and CH_4 (see Section 4) from process-based models. The bottom-up flux estimates are derived at high spatial resolution (~10 km) over Europe to be used in: 1) gridded flux estimates for prior information in the atmospheric inversions in WP3, and 2) national and sub-national annual GHG budgets for the synthesis in WP4 and 3) providing data for improving the understanding of key drivers for each GHG land flux and the impacts of ecosystem management (e.g. for crops, grasslands and forests) to the net annual fluxes in comparison to other drivers such as climate, atmospheric CO_2 and nitrogen deposition. Three ecosystem modelling frameworks are used to estimate the emissions: 1) LPJ-GUESS which is used to estimate the net ecosystem exchange (NEE) of CO_2 and soil N_2O emissions across natural, pasture, and crop ecosystems, 2) JSBACH-HIMMELI for estimating wetland, mineral soil and inundated land CH_4 emissions, and 3) ORCHIDEE which is used to estimate emissions of all three greenhouse gas components, CO_2, CH_4 and N_2O, from the European ecosystems.

Note that some of these data may be password-protected during a consolidation phase and thus only accessible to the EYE-CLIMA partners. However, after this phase, all data will be published in the Zenodo data repository and made available for everyone.

This project has received funding from the European Union's Horizon Europe research and innovation programme under grant agreement No 101081395

TABLE OF CONTENTS

This project has received funding from the European Union's Horizon Europe research and innovation programme under grant agreement No 101081395

1. Introduction

The objective of EYE-CLIMA deliverable D2.3 is to provide estimates of major GHG fluxes (CO_2, CH_4, and N_2O) from process-based models. The bottom-up flux estimates will be derived at high spatial (~10 km) and 3-hourly or daily temporal resolutions (depending on the model) over Europe to be used in: i) gridded flux estimates (with quantified uncertainties) for prior information in the atmospheric inversions in WP3, and ii) national and sub-national annual GHG budgets for the synthesis in WP4. Two state-of-the art models have been selected for each GHG, including one with multiple data-stream assimilation for CO2. The models will help assess the contribution to GHG fluxes from ecosystem subcomponents, such as above-ground versus below-ground, the split between different ecosystem types (forest, natural grassland, crops, peatland, etc) which will help to develop GHG reduction strategies. This is the first version of the dataset. A subsequent update of this deliverable will be provided during the course of the project.

2. Process modelling of LULUCF sector CO_2 fluxes for Europe

2.1 ORCHIDEE

Overall model description

ORCHIDEE (Organizing Carbon and Hydrology In Dynamic Ecosystems) is the Land Surface component of the Earth System Model - ESM from the Pierre Simon Laplace Institute (IPSL-CM6). It represents the dynamics governing the water, carbon, nitrogen, and energy balances of land ecosystems, following a process-based approach as much as possible. The modelling structures concentrates on several aspects: the exchanges of energy and water between the atmosphere and the biosphere (Ducoudré et al., 1993), and the carbon cycle dealing with photosynthesis, carbon allocation, litter decomposition, soil carbon dynamics, maintenance and growth respirations, plant phenology (Krinner et al., 2005) and a recent inclusion of carbon-nitrogen interactions (Zaehle and Friend, 2010; Vuichard et al., 2019).

The vegetation heterogeneity is described using fractions of 15 different plant functional types (PFTs Prentice et al., 1992) for each grid cell. All PFTs share the same equations but with different parameters, except for the leaf phenology. The annual evolution of the PFT maps (including a wood harvest product) is derived from the LUHv2 database (Lurton et al., 2020). In each grid cell, the PFTs are grouped into three soil tiles according to their physiological behaviour: high vegetation (forests) with eight PFTs, low vegetation (grasses and crops) with six PFTs, and bare soil with one PFT. An independent hydrological budget is calculated for each soil tile, to prevent forests from exhausting all soil moisture. In contrast, only one energy budget (and snow budget) is calculated for the whole grid cell. All components of the surface energy and water budgets, as well as plant/soil carbon fluxes, are computed at a sub-daily time step (i.e. 30 min) using a standard “big leaf” approach, but the “slow” processes (carbon allocation in the different plant reservoirs and litter and soil carbon dynamic) are computed on a daily time step. A physically based 11-layer soil hydrology scheme is used and vertical water fluxes are described using the Richard equation discretized with 11 layers for a 2 m soil depth, and a free drainage condition is imposed at the bottom of the soil column (de Rosnay et al., 2002; D'Orgeval et al., 2008). As detailed in Wang et al. (2016), the vertical discretization for heat diffusion is identical to that adopted for water up to 2 m. Furthermore, the soil depth for heat diffusion is extended to 90 m, with a zero-flux condition at the bottom and 18 calculation nodes. Finally, a three-layer snow scheme of intermediate complexity described in Wang et al. (2013) is included.

For the carbon cycle, photosynthesis depends on light availability, CO_2 concentration, soil moisture, and surface air temperature. It is parameterized based on Farquhar et al. (1980) and Collatz et al. (1992) for C_3 and C_4 plants, respectively. We used the implementation proposed by Yin and Struik (2009) that

This project has received funding from the European Union’s Horizon Europe research and innovation programme under grant agreement No 101081395

derives an analytical solution of the three equations linking the net assimilation rate, the stomatal conductance, and the intercellular CO_2 partial pressure. Once the carbon is fixed by photosynthesis, we compute the autotrophic respiration (growth and maintenance) and then allocate the remaining carbon into eight plant compartments (below and above ground sapwood and heartwood, leaves, fruit, roots, and reserves). Each compartment has a specific turnover depending on environmental stresses, and the living biomass is turned into a litter pool that is distributed in four compartments (metabolic or structural, both above or below ground). The litter is decomposed following first-order kinetics equations, modulated by upper soil moisture and temperature, with a fraction that is respired and a fraction that is distributed into three soil organic carbon pools (active, slow, and passive), following the CENTURY model (Parton et al., 1987). Each soil organic carbon pool is also decomposed following first-order kinetic equations modulated by soil moisture and temperature. Overall, the carbon respired from the litter and soil carbon pools defines the heterotrophic respiration.

Model version and configuration for EYE-CLIMA simulations

The model version that is used for the project is the one including the nitrogen cycle (ORCHIDEE-V3), which was described in Vuichard et al., (2019). This version is also the one that was used in the last two TRENDY model intercomparison for the global carbon budget (Friedlingstein et al., 2022). Key features of this version are:

- The nitrogen cycle, like the carbon cycle, is included at the PFT level.
- There is a parallel nitrogen pool for each carbon pool, with carbon to nitrogen (C:N) ratios varying throughout time.
- The C:N ratio at the leaf level varies as a result of nitrogen supply by roots and biomass allocation requirement.
- The C:N stoichiometry of the remaining live biomass pools (belowground and aboveground sapwood, belowground and aboveground heartwood, fruit, and fine roots) is determined by the C:N ratio of the leaves, but multiplied by a pool-dependent factor *fcn*.
- In terms of the Soil Organic Matter (SOM) decomposition, ORCHIDEE follows the scheme in which C/N ratios of SOM pools are expressed as a function of soil mineral nitrogen content (ammonium and nitrate).

More details on the nitrogen cycle with respect to the emissions of N_2O fluxes are provided in section 3.

The model is run for Europe with a dedicated forcing prepared for the project (see deliverable D2.1): a product based on the ERA5-land climate reanalysis of ECMWF (European Centre for Medium-Range Weather Forecast) with a bias correction using the Climate Research Unit (CRU) monthly dataset, at the spatial resolution of around 11 km. The simulations follow a protocol similar to the TRENDY protocol (Friedlingstein et al., 2022) but adapted for Europe. The model spin-up (procedure used to bring carbon pools to equilibrium) is performed by recycling the first 20 years of available atmospheric forcing (1901-1920) over the 340-years-long simulation with the CO_2 atmospheric concentration fixed to pre-industrial level (276.59 ppm, corresponding to the year 1700). PFT and land-use maps and Nitrogen inputs were prepared accordingly. The transient simulation is done for the years 1700-1900, still recycling the same forcing (1901-1920), but changing the CO_2-level and other inputs accordingly. Finally, the historical simulation is performed for 1901-2022 with time varying input data.

A data assimilation tool, ORCHIDAS, (https://orchidas.lsce.ipsl.fr/) has been used to optimize key parameters of the ORCHIDEE model using carbon- and nitrogen-related in-situ observations (eddy covariance and chambers). The system allows the optimization of selected parameters with multiple data streams, taking into account the different sources of uncertainty (parameter, model, observation) through a Bayesian framework. This version was optimized using carbon flux data collected on sites from the FLUXNET network. In addition, we have used manipulation experiment data from two Free Air

This project has received funding from the European Union's Horizon Europe research and innovation programme under grant agreement No 101081395

CO_2 Enrichment (FACE) experiments, to provide further constraints on vegetation response to increasing CO_2 by assimilating data under ambient and elevated CO_2 conditions. We found that we were able to improve the magnitude of modelled productivity simulated by this model version (Raoult et al., 2024).

Main results for CO_2 fluxes

A few results are presented below to illustrate the Net Biome Production (NBP) and the Gross Primary Production (GPP) simulated by ORCHIDEE over Europe. Figure 2.1.1 shows the spatial distribution of both NBP and GPP over the last decade. The spatial distribution of the GPP provides higher spatial heterogeneity following different climate conditions, nitrogen deposition and PFT distributions, while the NBP has a smoother spatial pattern. Overall, the western central part of Europe seems to have the largest carbon uptake. The highest GPP values seem to occur close to highly industrialised regions, where the nitrogen deposition and fertilisation are the highest.

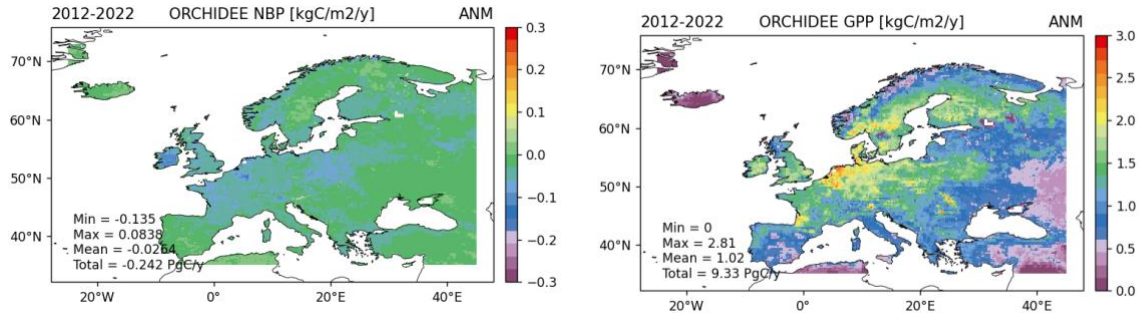

Figure 2.1.1: *Maps of simulated CO_2 fluxes from ORCHIDEE over Europe averaged over 2012 to 2022. Left: net biome production (net CO_2 flux including flux from harvested products) and right: Gross Primary Production (GPP).*

We then looked at the temporal evolution of the NBP (Figure 2.1.2) and the total values for the EU+3 (UK + Switzerland + Norway) in Table 2.1.1. Large variations of the annual NBP occur for all forest, grassland and cropland ecosystems. For the forests, variations between 40 and 100 TgC/yr are visible with very low carbon uptake in 2000, 2006, 2018 and 2022. These correspond mainly to drought conditions in Europe and large heat waves. For grassland, the variations range between 0 and 150 TgC/yr with more variation in the second decade (2010-2020) than the first decade (2000-2010) of the simulation. The years with low NBP do not correspond to the same years as for the forests. Cropland NBP oscillates between large carbon uptake (up to 100 TgC/yr) and a few years with negative NBP (a positive carbon flux to the atmosphere) up to -75 TgC/yr. The total NBB flux is on average a land carbon sink around 200 TgC/yr except for the year 2022 (-50 TgC/yr).

This project has received funding from the European Union's Horizon Europe research and innovation programme under grant agreement No 101081395

Table 2.1.1: *Total net biome production (net ecosystem exchange including also the harvest products; NBP TgC yr^{-1}) simulated by ORCHIDEE in forest, grassland, and cropland for EU27+3 (UK + Switzerland + Norway) countries between 2000-2022.*

Year	Forest TgC yr^{-1}	Grassland TgC yr^{-1}	Cropland TgC yr^{-1}	Total TgC yr^{-1}
2000	-31.8	-117.4	-3.5	-152.8
2001	-80.2	-118.4	-53.5	-252.0
2002	-100.8	-90.1	-68.5	-259.4
2003	-53.6	-107.0	74.8	-85.8
2004	-95.2	-100.7	-111.6	-307.5
2005	-40.4	-133.9	-17.1	-191.5
2006	-26.2	-81.4	-29.5	-137.1
2007	-111.5	-49.5	-75.8	-236.8
2008	-113.3	-84.1	-2.5	-199.9
2009	-109.9	-170.0	20.9	-259.0
2010	-82.9	-166.4	-70.5	-319.8
2011	-48.3	-11.6	-3.7	-63.6
2012	-54.7	-99.9	11.3	-143.2
2013	-73.5	-68.7	-66.0	-208.1
2014	-103.3	-1.5	-70.9	-175.7
2015	-82.0	-93.0	40.6	-134.3
2016	-83.7	-77.4	-55.6	-216.6
2017	-45.2	-139.8	-35.5	-220.4
2018	-27.4	-8.7	11.5	-24.5
2019	-49.8	-96.8	-6.1	-152.7
2020	-84.8	-37.6	-51.4	-173.8
2021	-97.9	-210.3	-78.3	-386.5
2022	-32.7	6.7	77.7	51.6

This project has received funding from the European Union's Horizon Europe research and innovation programme under grant agreement No 101081395

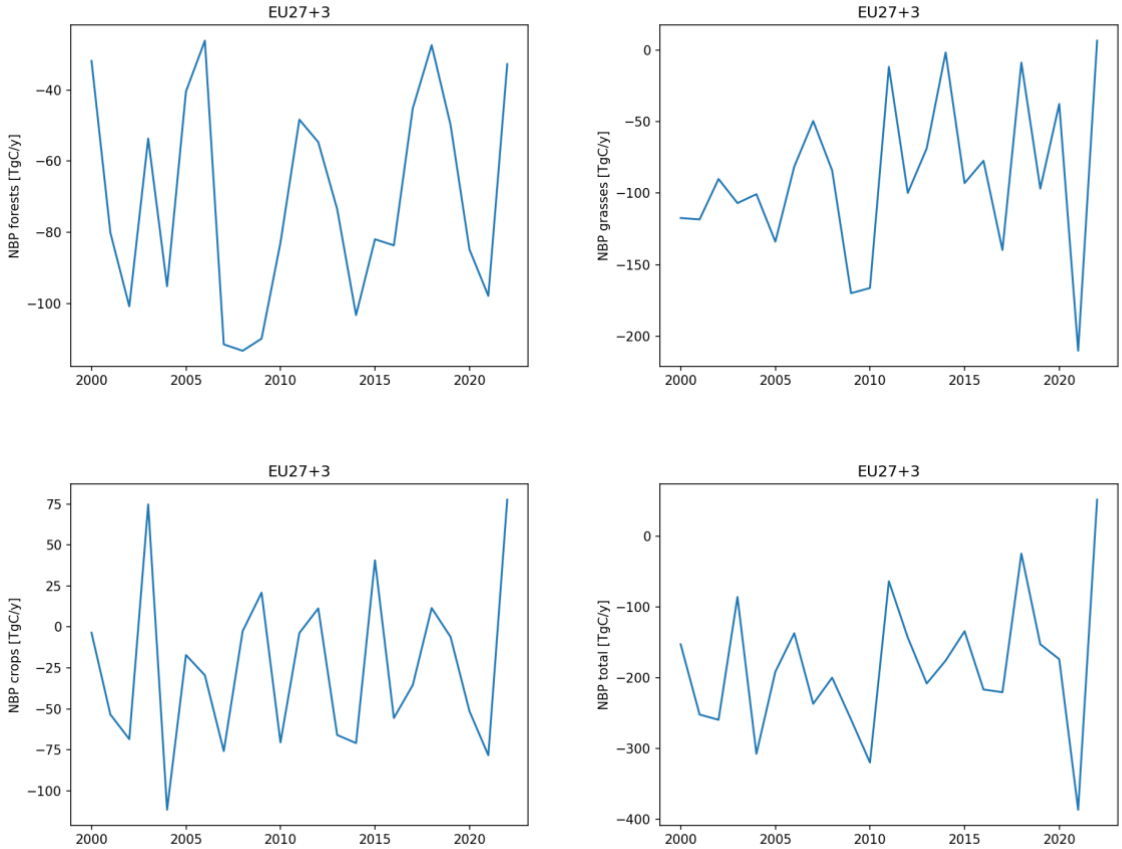

Figure 2.1.2: *Annual evolution of simulated net CO_2 fluxes (NBP) from ORCHIDEE over the EU27+3 (UK + Switzerland + Norway) for the forest (upper left), grassland (upper right) and cropland ecosystems (lower left), as well as for the total flux (lower right).*

2.2 LPJ-GUESS

LPJ-GUESS is a process-based global vegetation model that can be used to investigate plant and soil C-N dynamics and their interactions in response to changes in environment (e.g., climate, atmospheric CO_2 levels, and N deposition) and management (e.g., crop type, N fertilizer, and harvest) through simulating individual- and patch-level plant physiological and biogeochemical processes on a daily time step (Smith et al., 2014). Natural vegetation implemented in the model is characterized by 12 plant functional types (PFTs), with ten woody and two herbaceous types included. PFTs differ in their phenology, photosynthetic pathway (C_3 or C_4), growth strategy, and bioclimatic limitations. Pastures are represented by competing C_3 and C_4 grass PFTs, with half of aboveground biomass harvested annually to represent grazing impacts (Lindeskog et al., 2013). Within the EYE-CLIMA framework, six crop functional types (CFTs)—two temperate C_3 crops with spring and autumn sowing dates, a tropical C_3 crop representing rice, a C_4 crop representing maize, and two N-fixing grain legumes representing soybean and pulses—are simulated to represent croplands over Europe, with crop-specific differences in morphological traits, dynamic C-N allocation patterns, heat requirements for growth, and N fertilization management (Olin et al., 2015; Ma et al., 2022a). Due to the absence of crop-specific calendar information for high-resolution simulations over Europe, the sowing date in each grid cell depends on a set of rules driven by crop- and climate-specific characteristics, with five seasonality types represented (see Waha et al., 2012 for details). Crops are harvested annually when the dynamic potential heat units (i.e., accumulated degree-days above a base temperature for each CFT) are fulfilled (Olin et al., 2015).

This project has received funding from the European Union's Horizon Europe research and innovation programme under grant agreement No 101081395

Managed forests, such as clear-cutting and thinning intensity (e.g. Lindeskog et al., 2021), have not been included in this first round of simulations.

Model spin-up follows the protocol in Ma et al. (2022a). All simulations are initialized with a 500-year spin-up using atmospheric carbon dioxide (CO_2) concentration from 1901 and repeating de-trended climate from 1901-1930. During spin-up, potential natural vegetation is simulated for the first 470 years, and then the cropland fraction linearly increases from zero to the first historic value (1901) in the last 30 years. Monthly atmospheric N deposition simulated by CCMI (NCAR Chemistry-Climate Model Initiative) from 1901 to 2022 is used and interpolated to the same resolution of the climate forcing (0.1°×0.1°; see below for details) (Tian et al., 2018).

The model experiment starts with the year 1901 and runs throughout the historical period till 2022 after model spin-up, with standard cropland managements (i.e., conventional tillage, 25% of residue retention, N fertilizer and manure application, and no cover crops; Olin et al., 2015), unfertilized pasture, and unmanaged natural vegetation simulated. The model is driven by daily mean air temperature, precipitation, solar radiation, relative humidity, and wind speed from the observation-based CRU-ERA5 data set, spanning from 1901-2022 at 0.1° resolution. Annual atmospheric CO_2 concentration is from Meinshausen et al. (2020). Historical land use/land cover input data between 1901 and 2020 are adopted from HILDA+ (Winkler et al., 2021) and are aggregated from 0.01° to 0.1° with fractions of natural vegetation, pasture, and cropland given for each grid cell. The growth distribution of various crop types, distinguishing shares of rain-fed and irrigated crop-specific fraction per grid cell, is based on the MIRCA data set around the year 2000 (Portmann et al., 2010) and aggregated to the six CFTs simulated over Europe. Thus, although the total cropland area at each grid cell varied annually over the simulation period, the relative fraction of each CFT within that cropland area remained static. In terms of N fertilization, CFT-specific industrial N fertilizer and manure inputs are derived from the HaNi data set (Tian et al., 2022), ranging from 1901-2019 at 0.1° resolution. Since information on the timing of N fertilization in crops across Europe does not exist, in LPJ-GUESS we assume that synthetic N fertilizer is added to the soil mineral N pool for plant uptake at three crop development stages, with varying application rates for each CFT (Olin et al., 2015; Ma et al., 2022b). Manure is applied as a single input to cropland at sowing to account for the time required for manure N to be made available for crops. As soil input, a soil map with fractions of clay, silt, and sand from the WISE30sec data set (Batjes, 2016) is used to parameterize soil hydraulic properties. For the first-round deliverable within the EYE-CLIMA framework, the three CO_2 flux components: net primary productivity (NPP), heterotrophic respiration (Rh), and net ecosystem exchange (NEE), together with soil N_2O emissions across natural, pasture, and crop ecosystems (see Sect. 3.2 below for details), are computed and provided in EU27+3 countries with a daily time step.

The European CO_2 fluxes from the terrestrial ecosystems simulated by LPJ-GUESS are shown as a map in Figure 2.2.1 and as time series between 1951-2022 in Fig. 2.2.2, with the annual total NEE over the recent two decades given in Table 2.2.1. Low NPP and Rh in natural ecosystems are found in the southern and northern parts of Europe (such as Spain, Portugal, and Norway), with simulated values ranging from 0-0.2 kgC m^{-2} yr^{-1}. In contrast, the modelled NPP in west and east EU is as high as 0.5-0.8 kgC m^{-2} yr^{-1}, most likely due to the warm and moist climate during the summer time. NEE, as the difference between Rh and NPP in LPJ-GUESS, shows a more complex spatial pattern in the recent decade: the biogenic flux present a stronger sink of CO_2 in west and east EU (-0.2 to -0.15 kgC m^{-2} yr^{-1} of NEE), in comparison with the NEE range of -0.05 to 0.05 kgC m^{-2} yr^{-1} in some parts of southern and northern EU, where the natural vegetation is close to being carbon neutral or even a carbon source (Fig. 2.2.1).

CO_2 fluxes show an increasing (NPP and Rh) or decreasing (NEE) trend over the simulation period, but with large variability between individual years (Fig. 2.2.2). Natural vegetation, pasture and cropland are simulated as a strong CO_2 sink, a neutral ecosystem, and a weak CO_2 source in European terrestrial

This project has received funding from the European Union's Horizon Europe research and innovation programme under grant agreement No 101081395

ecosystems between 2000-2022, respectively, with the simulated total NBP of -102±58 (mean ± 1 standard deviation), 3±27, and 89±12 TgC yr^{-1} for the three land-use types. Net carbon emission of the entire land ecosystems in the LPJ-GUESS experiments is stronger in drought years (e.g., 126 and 157 TgC for the year 2003 and 2022, respectively) in comparison with the mean uptake of -10±85 TgC yr^{-1} calculated between 2000-2022 (Table 2.2.1).

Table 2.2.1: *Total net biome production (NBP; TgC yr^{-1}) simulated by LPJ-GUESS in natural vegetation, pasture, and cropland for EU27+3 countries between 2000-2022.*

Year	Natural TgC yr^{-1}	Pasture TgC yr^{-1}	Cropland TgC yr^{-1}	Total TgC yr^{-1}
2000	-30.4	7.3	108.2	85.1
2001	-35.7	1.3	96.3	61.9
2002	-183.9	-22.0	102.5	-103.4
2003	-18.6	41.5	102.5	125.5
2004	-175.0	-24.8	71.3	-128.5
2005	-61.8	12.4	97.0	47.6
2006	-74.7	25.6	106.2	57.1
2007	-155.2	-57.1	87.9	-124.4
2008	-201.1	-6.8	86.0	-121.9
2009	-116.1	19.4	90.8	-5.8
2010	-150.5	-2.0	78.9	-73.5
2011	-95.2	10.3	100.2	15.3
2012	-60.0	-2.0	82.1	20.0
2013	-104.4	25.9	83.6	5.2
2014	-184.7	-36.0	96.4	-124.2
2015	-103.1	35.6	86.8	19.4
2016	-95.9	-25.9	81.6	-40.2
2017	-57.5	9.8	93.4	45.7
2018	-77.5	30.7	99.5	52.6
2019	-138.2	-6.5	72.4	-72.2
2020	-78.2	4.4	72.8	-1.0
2021	-158.2	-22.6	69.5	-111.3
2022	12.3	54.3	90.8	157.4

This project has received funding from the European Union's Horizon Europe research and innovation programme under grant agreement No 101081395

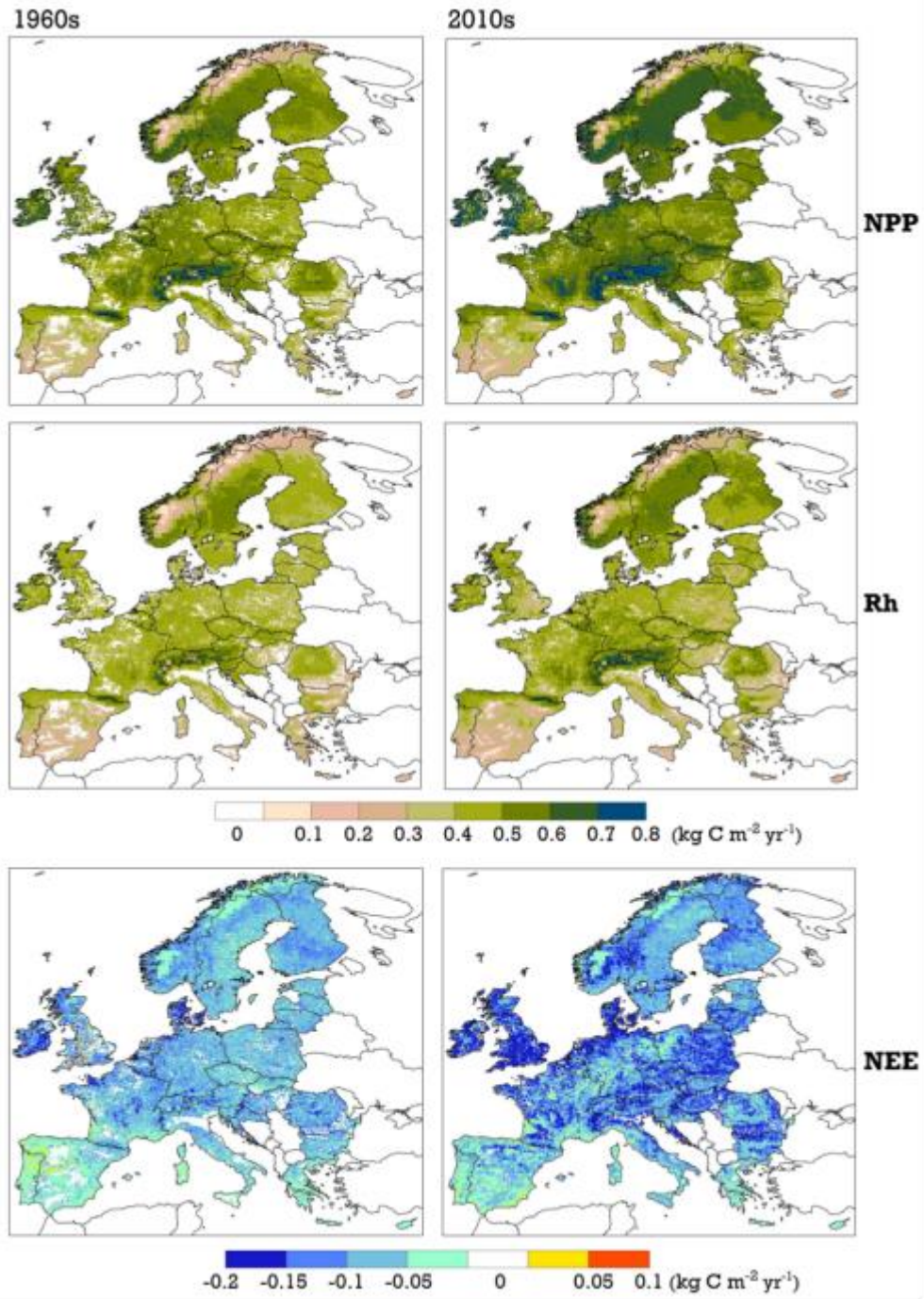

Figure 2.2.1: *Maps of simulated CO_2 fluxes in natural vegetation by LPJ-GUESS over EU27+3 countries, averaged over 1960s and 2010s.*

This project has received funding from the European Union's Horizon Europe research and innovation programme under grant agreement No 101081395

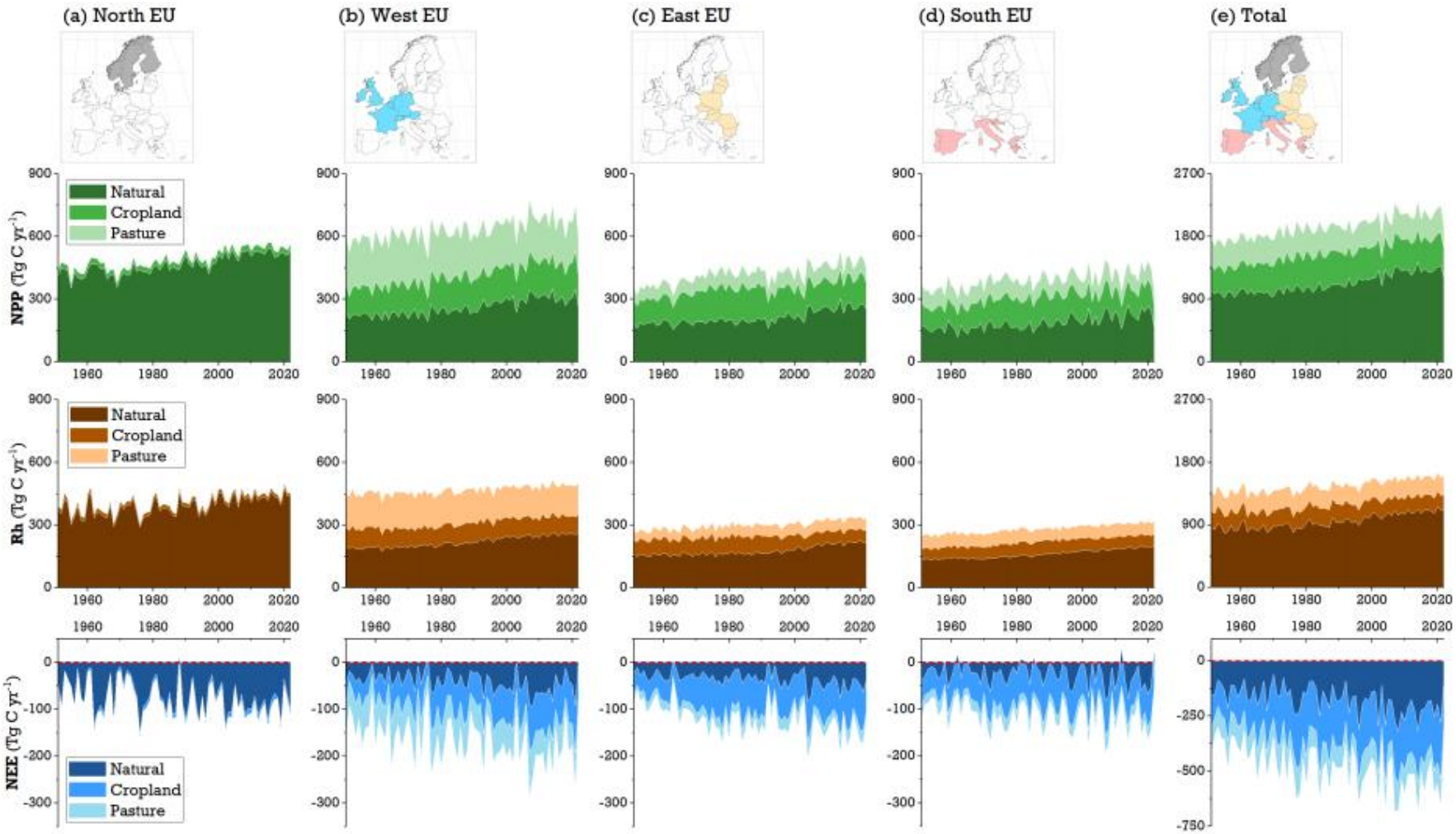

Figure 2.2.2: *Simulated total annual CO_2 fluxes (Tg C yr^{-1}) in natural vegetation, pasture, and cropland by LPJ-GUESS over EU27+3 countries between 1951-2022.*

This project has received funding from the European Union's Horizon Europe research and innovation programme under grant agreement No 101081395

2.3 Comparison between ORCHIDEE and LPJ-GUESS CO_2 fluxes

This section is a first step toward the quantification of the CO_2 flux uncertainty with a comparison of the net biome production (net flux) between the two models. Most results can be found under the webpage: https://orchidas.lsce.ipsl.fr/dev/divers/eye-clima2.php

Figure 2.3.1 shows the spatial distribution of the NBP for the two models as well as their difference. We clearly see that LPJ-GUESS NBP has a much larger spatial heterogeneity than ORCHIDEE with values spanning the range -0.3 to 0.3 KgC/m^2/yr while ORCHIDEE NBP values range only between -0.1 and 0.15 KgC/m^2/yr. On average over the period 2012 - 2022, most regions show a larger carbon uptake in ORCHIDEE than in LPJ-GUESS. The map of difference between the two models (Figure 2.3.1, lower panel) indicates that on average for central and West Europe ORCHIDEE simulates a much larger C sink while LPJ-GUESS simulates a larger sink in the north (Scandinavia).

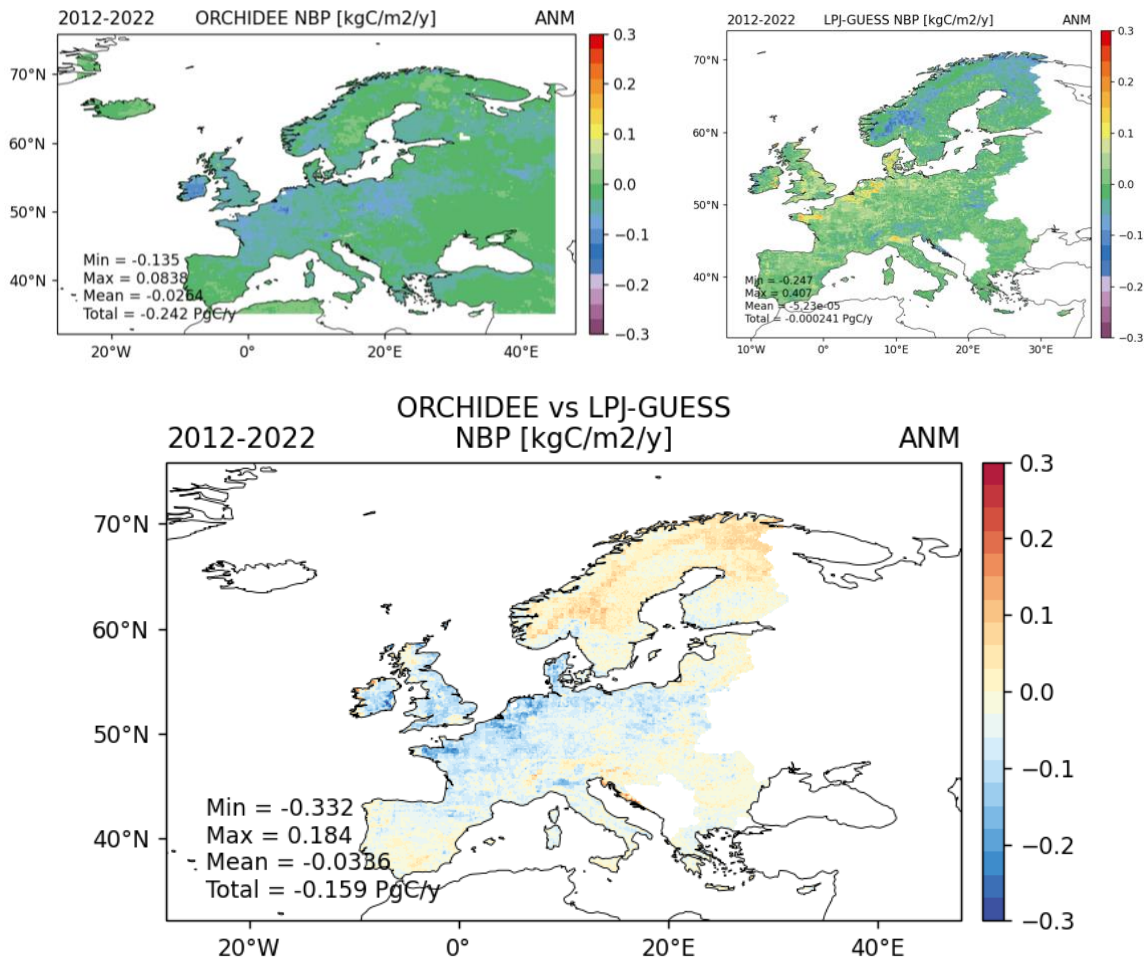

Figure 2.3.1: *Maps of simulated net CO2 fluxes (NBP) from ORCHIDEE (top left), LPJ-GUESS (top right) and the difference between ORCHIDEE and LPJ-GUESS (bottom) over Europe averaged over 2012 and 2022.*

If we focus on the year-to-year NBP variations, Figure 2.3.2 shows these variations for the EU27+3 (UK + Switzerland + Norway) and three individual countries (France, Germany and Norway). ORCHIDEE presents for almost all years a negative NBP (net carbon uptake) for EU27+3 and the selected countries, with however a few years (2018 and 2022) with large anomalies turning the net ecosystem carbon uptake to a small source (example of France and Germany in 2022 and Germany in 2018). On

This project has received funding from the European Union's Horizon Europe research and innovation programme under grant agreement No 101081395

the other hand, LPJ-GUESS simulates lower or positive NBP (equivalent to a carbon source), when averaged at country or groups of countries level, depending on the year. However, the year-to-year variations of LPJ-GUESS NBP are more in line with those from ORCHIDEE, especially for the big summer heat wave in 2022. Reasons for the differences between the mean flux of the two models are under investigation and will be discussed in the version of comparison.

Figure 2.3.2: *Annual evolution of simulated net CO_2 fluxes (NBP) from ORCHIDEE and LPJ-GUESS from 2012 to 2022 for four regions; top-left: EU27+3 (UK + Switzerland + Norway); top-right: France; bottom left: Germany; bottom-right: Norway.*

3. Process modelling of agricultural and forest land N_2O fluxes for Europe

3.1 ORCHIDEE

N cycle model description

The main features of the ORCHIDEE model are described in the section above for the CO_2 fluxes (section 2.1). Here, we thus only briefly describe the C-N dynamics that lead to the emissions of N_2O fluxes. Modeling of the mineral N dynamics by the ORCHIDEE model originates from the formulations used in the O-CN (Zaehle and Friend, 2010). It is composed of five pools for ammonium/ammoniac, nitrate, NOx, nitrous oxide, and di-nitrogen forms. N_2O production in both nitrification and denitrification processes are represented. To be able to simulate co-occurring nitrification and denitrification processes in aerobic and anaerobic microsites, the soil is differentiated into aerobic and anaerobic fractions based on an empirical relationship linking oxygen consumption due to soil respiration (both belowground autotrophic and heterotrophic) and oxygen diffusion into the soil, which is itself functions of soil moisture [Li et al., 2000] and soil temperature. The potential daily rate of

This project has received funding from the European Union's Horizon Europe research and innovation programme under grant agreement No 101081395

nitrification (Rnit) occurs only on the aerobic fraction of the soil and is a function of temperature, pH, and ammonium concentration (C_{NH4}):

$$R_{nit} = (1 - f(WFPS))\ f(T1)\ f(pH1)\ k_{nit}\ C_{NH4}$$

where k_{nit} is the reference potential NO_3^- production per mass unit of ammonium.

Mineral nitrogen inputs in the soil-plant system are related to:

- Atmospheric nitrogen deposition in the form of NHx and NOy components
- Biological nitrogen fixation (BNF) on any land category. The BNF rates are calculated as a function of evapotranspiration using the (Cleveland et al., 1999) method. In particular, all simulations employ a single evapotranspiration climatology based on a worldwide ORCHIDEE simulation for present-day conditions
- Nitrogen fertilization on croplands.

These inputs data were taken from the NMIP model intercomparison project (Tian et al., 2018).

ORCHIDEE N_2O fluxes

Figure 3.1.1 displays the spatial distribution of the total N2O fluxes across Europe as simulated by ORCHIDEE for the last decade (2012-2022), while Figure 3.1.2 reveals the temporal evolution for the EU27+3 (UK, Switzerland, Norway) of the total flux and the contributions from grassland, cropland and forests. The mean flux across geographical Europe is around 0.129 gN/m^2/yr, with a large peak around the most industrialised regions of Europe (i.e., the Netherlands) where the N deposition and fertilisation is the largest. The total flux for the EU27+3 is around 0.7 TgN/yr while for geographical Europe (the domain of Figure 3.1.1) it is around 1.2 TgN/yr. The temporal evolution of the total N2O flux. Total forest fluxes are two times smaller than the cropland and grassland fluxes. Both cropland and forest fluxes show a small decrease after 2010 due to reduction of N fertilizer use for cropland. The grassland fluxes show a spurious increase in 2020-2022 that is under investigation.

Finally, Table 3.1.1, displays the total fluxes for the three ecosystem types from 2000 to 2022. Additional plots are also available under: https://orchidas.lsce.ipsl.fr/dev/divers/eye-clima2.php

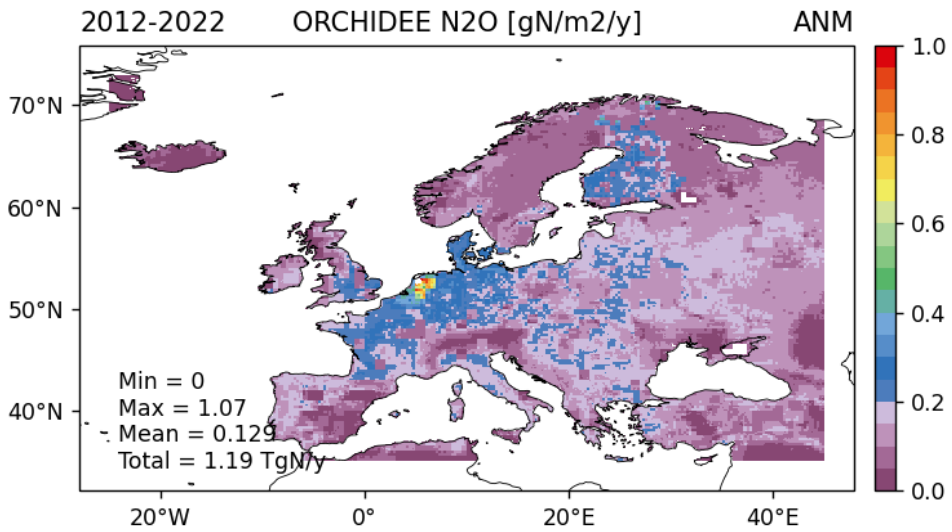

Figure 3.1.1: *Maps of simulated N_2O emissions for all ecosystems by ORCHIDEE over EU27+3 countries, averaged over 2012 and 2022.*

This project has received funding from the European Union's Horizon Europe research and innovation programme under grant agreement No 101081395

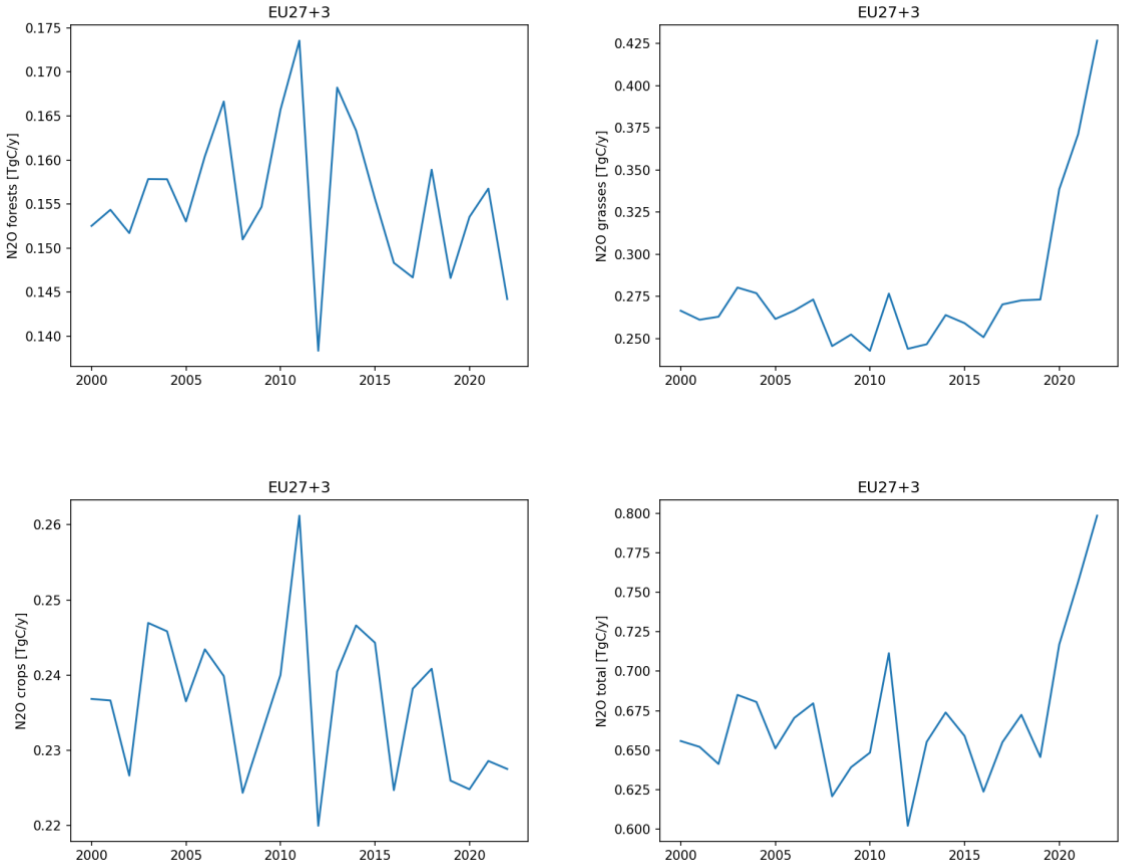

Figure 3.1.2: *Annual evolution of simulated N_2O emissions from ORCHIDEE over the EU27+3 (UK + Switzerland + Norway) for the forest, grassland and cropland ecosystems, as well as for the total flux.*

3.2 LPJ-GUESS

Soil C-N dynamics in LPJ-GUESS are simulated by a soil organic matter (SOM) scheme derived from the Century model (Parton et al., 1993), in which SOM and litter are characterized by 11 pools with prescribed C:N ratios and decay rates (Smith et al., 2014). The transfer of SOM between pools drives N mineralization or immobilization, as a result of the altered C:N ratios in the donor and receiver pool. Net N mineralization (i.e., mineralization minus immobilization), together with industrial N fertilizer and atmospheric N deposition, determine the size of the total soil mineral N pool, which is depleted by plant N uptake, as well as by ecosystem N losses through N leaching and gaseous N emission on a daily time step (Zaehle & Friend, 2010; Wårlind et al., 2014). Gaseous N emission produced in the soil to the atmosphere is simulated as NH_3, NO, N_2O, and N_2, with the representation of soil N dynamic processes including ammonification, nitrification, and denitrification in the SOM pools. Within the EYE-CLIMA framework, we update a detailed representation of soil N transformation scheme adopted from the DyN model (Xu-Ri & Prentice, 2008) and the CLM5 model (Val Martin et al., 2023).

Microbial processes in soils occur on short timescales and spatially in a highly heterogeneous pattern. The daily time-step in LPJ-GUESS and the 10' spatial resolution make it difficult to represent all critical processes in the required detail. A number of factors influence the nitrification and denitrification rates where the processes are not fully understood, and where the influence of the major controlling factors is not easily defined; factors can have multiple roles and interact with other factors. Nonetheless, soil NO, N_2O, and N_2 emissions are known to be controlled by soil characteristics such as drainage (aeration, texture, compaction), temperature, moisture, *pH*, organic matter, available N (NH_4 and NO_3), and C:N ratios of soil organic matter.

This project has received funding from the European Union's Horizon Europe research and innovation programme under grant agreement No 101081395

Table 3.1.1: *Total soil N_2O emissions (TgN yr^{-1}) simulated by ORCHIDEE in forest vegetation, grassland, and cropland for EU27+3 countries between 2000-2022.*

Year	Forest TgN yr^{-1}	Grassland TgN yr^{-1}	Cropland TgN yr^{-1}	Total TgN yr^{-1}
2000	0.153	0.267	0.237	0.656
2001	0.154	0.261	0.237	0.652
2002	0.152	0.263	0.227	0.641
2003	0.158	0.280	0.247	0.685
2004	0.158	0.277	0.246	0.681
2005	0.153	0.262	0.237	0.651
2006	0.160	0.267	0.243	0.670
2007	0.167	0.273	0.240	0.680
2008	0.151	0.246	0.224	0.621
2009	0.155	0.252	0.232	0.639
2010	0.166	0.243	0.240	0.649
2011	0.174	0.277	0.261	0.711
2012	0.138	0.244	0.220	0.602
2013	0.168	0.247	0.240	0.655
2014	0.163	0.264	0.247	0.674
2015	0.156	0.259	0.244	0.659
2016	0.148	0.251	0.225	0.624
2017	0.147	0.270	0.238	0.655
2018	0.159	0.273	0.241	0.672
2019	0.147	0.273	0.226	0.646
2020	0.154	0.339	0.225	0.717
2021	0.157	0.371	0.229	0.757
2022	0.144	0.427	0.228	0.798

We implemented these limiting factors to nitrification and denitrification, following empirical relationships between gaseous N emissions and environmental control factors established in field experiments (e.g., Weier et al., 1993; Maag & Vinther, 1996; Rochester, 2003; Liu et al., 2010; Wagena

This project has received funding from the European Union's Horizon Europe research and innovation programme under grant agreement No 101081395

et al., 2017; Blanc-Betes et al., 2021; Zhang et al., 2023). More details on the soil N transformation in LPJ-GUESS will be provided in a forthcoming manuscript and, therefore, are not presented here.

European soil N_2O emissions from land ecosystems simulated by LPJ-GUESS are shown as a map in Figure 3.2.1 and as time series between 1951-2022 in Figure 3.2.4. The largest N_2O emissions from natural vegetation is found in central and east Europe, where the simulated rates are as high as 7.0 kgN ha^{-1} yr^{-1}; in comparison, the north Europe with cold climates shows less N emissions of 0 to 1.0 kgN ha^{-1} yr^{-1}, probably due to the slow turnover of the SOM pools in the high latitudes. Chemical N fertilizer application rate in the model simulation plays an important role in controlling N_2O emissions in European cropland, with the greatest fluxes found the highly fertilized soils (e.g., France, Germany, and UK); while the regions with less N inputs, such as Baltic countries, generally present a weaker N_2O source (Figure 3.2.2).

Natural vegetation is simulated as the main N_2O contributor (61%) to the total emissions in European terrestrial ecosystems between 2000 and 2022, followed by cropland (32%) and pasture (7%), with the estimated emissions of 0.46 ± 0.05, 0.24 ± 0.03, and 0.05 ± 0.01 TgN yr^{-1} for the three land-use types, respectively (Table 3.2.1). We also found that the modelled total N_2O from the European cropland shows a declining trend between 2000-2022 (Fig. 3.2.2), mainly as a result of reduced N fertilizer use in the past two decades. Compared with the high N_2O emissions from natural vegetation and cropland, the pasture ecosystem in our simulations in general displays as a weaker N_2O source. Manure application in pasture, which is a common management practice in Europe, has not yet been included in the current model version.

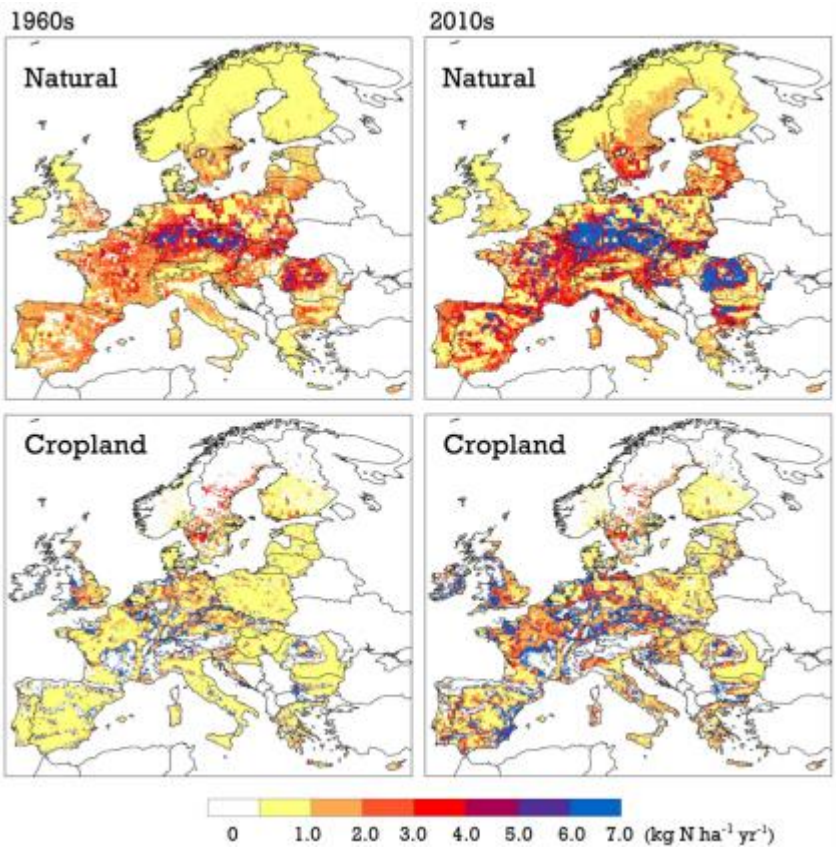

Figure 3.2.1: *Maps of simulated N_2O emissions in natural vegetation and cropland by LPJ-GUESS over EU27+3 countries, averaged over 1960s and 2010s.*

This project has received funding from the European Union's Horizon Europe research and innovation programme under grant agreement No 101081395

Table 3.2.1: *Total soil N_2O emissions (TgN yr^{-1}) simulated by LPJ-GUESS in natural vegetation, pasture, and cropland for EU27+3 countries between 2000-2022.*

Year	Natural TgN yr^{-1}	Pasture TgN yr^{-1}	Cropland TgN yr^{-1}	Total TgN yr^{-1}
2000	0.358	0.034	0.295	0.687
2001	0.444	0.056	0.275	0.775
2002	0.498	0.059	0.295	0.852
2003	0.361	0.038	0.225	0.624
2004	0.383	0.056	0.240	0.679
2005	0.476	0.047	0.245	0.768
2006	0.500	0.066	0.264	0.830
2007	0.563	0.071	0.311	0.945
2008	0.450	0.043	0.230	0.723
2009	0.436	0.037	0.210	0.683
2010	0.505	0.058	0.228	0.791
2011	0.403	0.042	0.221	0.666
2012	0.406	0.047	0.212	0.665
2013	0.469	0.056	0.205	0.730
2014	0.539	0.063	0.259	0.861
2015	0.464	0.047	0.214	0.725
2016	0.467	0.050	0.208	0.725
2017	0.445	0.048	0.223	0.716
2018	0.443	0.054	0.219	0.716
2019	0.438	0.050	0.220	0.708
2020	0.509	0.064	0.222	0.795
2021	0.527	0.054	0.202	0.783
2022	0.491	0.036	0.197	0.724

This project has received funding from the European Union's Horizon Europe research and innovation programme under grant agreement No 101081395

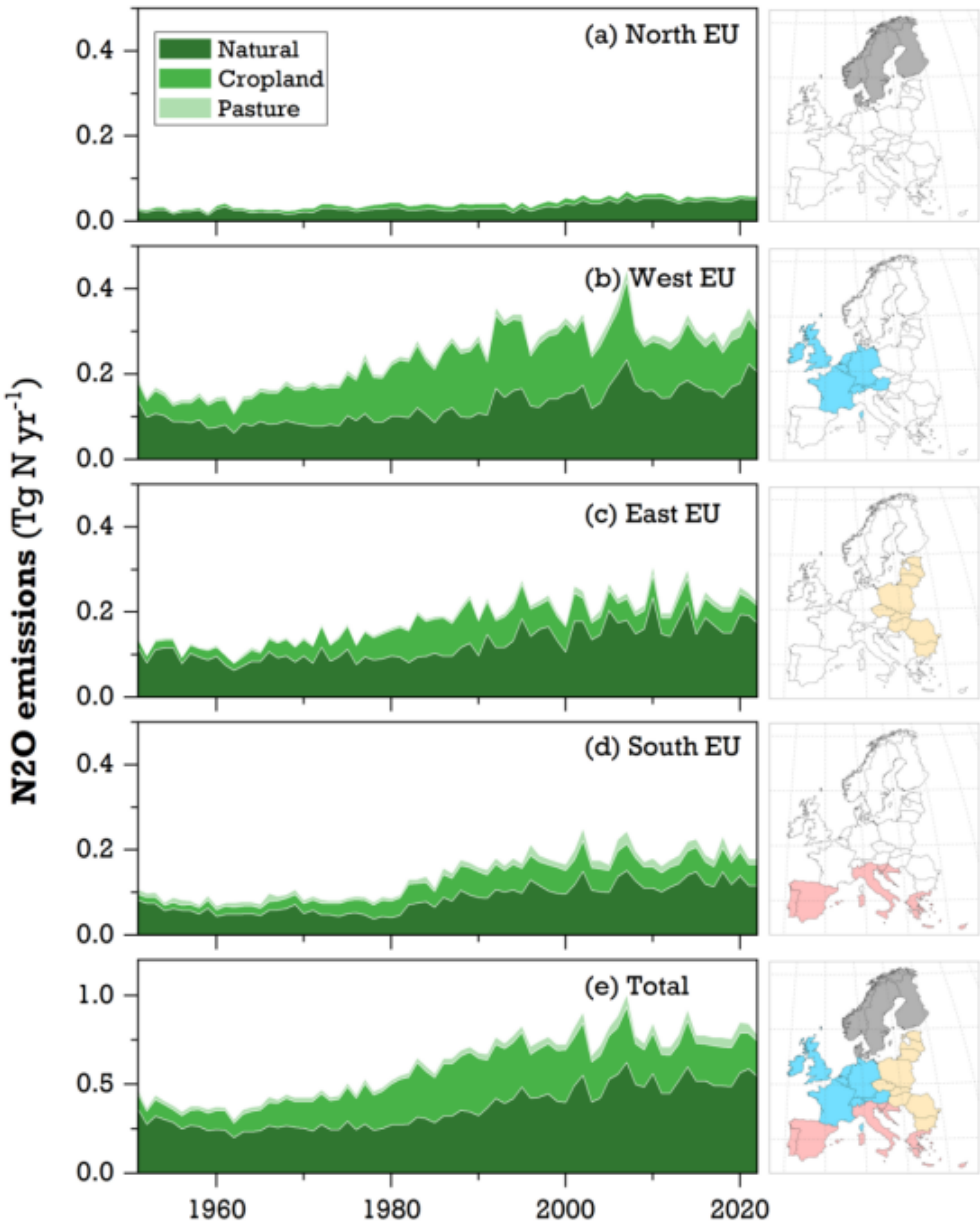

Figure 3.2.2: *Simulated total annual N_2O emissions (Tg N yr^{-1}) in natural vegetation, pasture, and cropland by LPJ-GUESS over EU27+3 countries between 1951-2022.*

3.3 Comparison between ORCHIDEE and LPJ-GUESS N_2O fluxes

As for CO_2, this section is a first step toward the quantification of the N_2O flux uncertainty with a comparison of the net biome production (net flux) between the two models. Figures 3.3.1 and 3.3.2 compare the spatial distribution and the temporal evolution of the total N_2O fluxes, respectively.

On average the two models produce similar total flux for Europe with, however, some differences in the spatial and temporal distributions. The hotspot of emission around the Netherlands in ORCHIDEE is not found in LPJ-GUESS, while LPJ-GUESS has larger emission in Germany and Poland associated with cropland areas. On average ORCHIDEE has slightly larger N_2O fluxes in the northern countries, especially for the forest ecosystems. The year-to-year variations of these fluxes are also different between the two models, LPJ-GUESS showing slightly larger variations than ORCHIDEE (Fig. 3.3.2). ORCHIDEE shows a

This project has received funding from the European Union's Horizon Europe research and innovation programme under grant agreement No 101081395

positive trend in N_2O emissions for the EU27+3 (UK + Switzerland + Norway) but not for all countries (i.e. Germany shows no increasing emissions). On the other hand, LPJ-GUESS does not show any significant trend. We do not see strong correlation between the year-to-year variations of the ORCHIDEE and LPJ-GUESS fluxes. All these differences are currently under investigation.

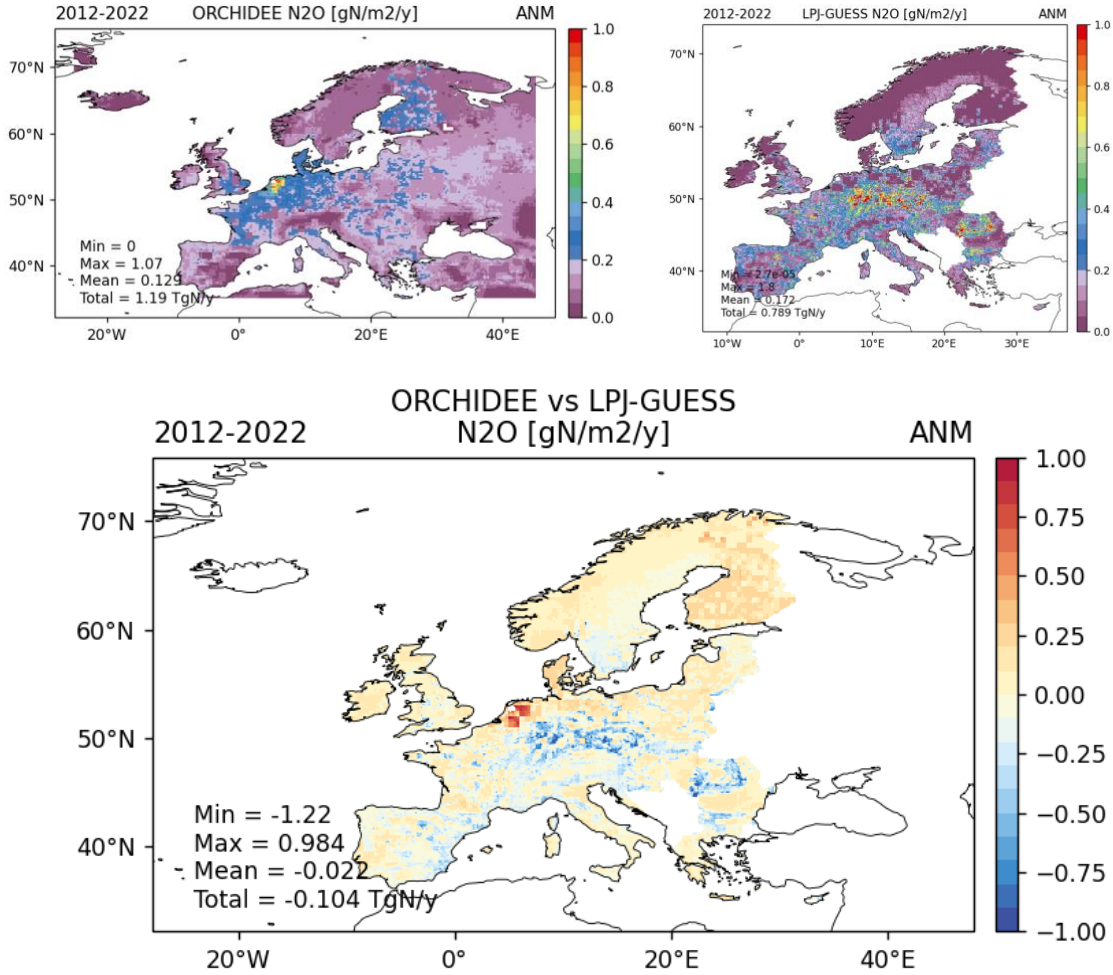

Figure 3.3.1: *Maps of simulated N_2O emissions from ORCHIDEE (top left) and LPJ-GUESS (top right) over Europe averaged over 2012 and 2022 with the difference map between the models (bottom).*

This project has received funding from the European Union's Horizon Europe research and innovation programme under grant agreement No 101081395

Figure 3.3.2: *Annual evolution of simulated N_2O emissions from ORCHIDEE and LPJ-GUESS from 2012 to 2022 for four regions; top-left: EU27+3 (UK + Switzerland + Norway). Top-right: France; Bottom left: Germany; Bottom-right: Norway.*

4. Process modelling of natural CH_4 fluxes for Europe

4.1 JSBACH-HIMMELI

Natural terrestrial CH_4 flux comprises four terms: peatland soil emission, wet mineral soil emission, dry mineral soil uptake and seasonally inundated soil emission. The peatlands, inundated lands and mineral lands together cover the land area of a grid cell. Peatland extent is considered here as a conservative, static fraction of the grid cell area, and inundated land has variable extent. For methane emission calculations, peatland extent is first subtracted from the inundated land extent (WAD2M, Zhang et al., 2021), and JSBACH-HIMMELI model is used for calculation of peatland fluxes. The remaining inundated land extent is used for calculation of inundated land emissions with a semi-empirical parameterization (Spahni et al, 2011) utilising JSBACH input. The mineral land extent comprises the remains of the grid cell land area after subtracting the joint peatland and inundated land areas, and mineral land fluxes are estimated using approaches by Spahni et al. (2011) and Curry et al. (2017). The land cover input data for methane emission modelling is described in EYE-CLIMA D2.2 including the vegetation and soil type mapping for JSBACH model as well as inundated land maps.

JSBACH-HIMMELI is a combination of two models, a land-surface model JSBACH (Reick et al 2013), and HIMMELI (HelsinkI Model of MEthane buiLd-up and emIssion for peatlands; Raivonen et al., 2017), which is a specific model for northern peatland emissions of CH_4. JSBACH simulates soil hydrology, vegetation gas exchange and soil carbon input and decay both in oxic and anoxic soil conditions and provides HIMMELI with soil temperature, water table depth, the leaf area index and anoxic respiration

This project has received funding from the European Union's Horizon Europe research and innovation programme under grant agreement No 101081395

from waterlogged soil carbon storages. Decomposition of soil carbon provides substrate for methane production and thus anoxic soil respiration rate is needed to estimate CH_4 fluxes. Simulations of water table level are used for solving the anoxic and oxic layers of the soil column and methane production, oxidation, diffusion and plant transport processes are simulated in those layers.

The parameterisation by Spahni et al (2011) has been applied for calculating methane emissions from the inundated mineral soils, utilising heterotrophic soil respiration rate from JSBACH and a conversion factor for methane emissions. For non-inundated upland mineral soils the wet mineral soil methane emissions have been calculated using heterotrophic soil respiration rate from JSBACH, a conversion factor for methane, and a rate limitation utilising an empirical soil moisture threshold for mineral soil methane emissions. Dry soil methane uptake rates have been calculated following the Curry (2017) scheme for microbial methane oxidation using soil moisture, soil temperature and soil respiration data produced by JSBACH as input.

CRU-ERA5 climate data have been used to drive JSBACH-HIMMELI in a 0.1 × 0.1 degree resolution grid covering Europe in a rectangular domain (Fig. 4.1.1). The CRU-ERA5 data was re-gridded to 0.1 × 0.1 degree resolution from original 0.125 degree resolution. JSBACH peat carbon storages were accumulated in a spin-up run. The decay of waterlogged peat is slower than decay of carbon in upland soils and many natural peatlands in northern Europe have been accumulating carbon over a long climate period and currently continue accumulation. For most of the region equilibrium was not reached after 2500 years of spin-up, however at that stage the mean peat depth was around two meters, which is quite realistic for north European pristine peatlands. Thus, the soil state after 2500 years of spin-up was accepted as the initial state in JSBACH-HIMMELI CH4 forward simulations, running from year 2000 to 2022. The four methane flux components have been calculated in daily time resolution.

Peatlands

The European peatland methane fluxes are shown as a map in Figure 4.1.1 and as monthly time series over years 2000 – 2022 in Figure 4.1.2. The annual peatland emissions are given together with the other components in Table 4.1.1 and shown as time series in Figure 4.1.3. The distribution of the peatland emissions follows the peatland map created based on the EU-CORINE land use map, with CORINE “bog” and “inland marsh” categories specifying the peatland locations. Mean annual total maps (Fig. 4.1.1) show less emission in the southern parts of Europe and more emission in the north where peatlands are mostly located, as seen in the high-resolution mapping over the EU-27 countries.

Year-to-year and seasonal variability of the flux components is controlled by meteorological drivers and shows a clear seasonal cycle (Fig. 4.1.2 and Fig 4.1.3). The peatland emissions show high summer-time peak monthly totals, and low winter-time emissions due to freezing temperatures in the north where peatlands are mostly located. The magnitude of the emissions is sensitive to, e.g., simulated peat water table depth, temperature profile and fresh substrate input from peatland vegetation. Peatland emissions are the largest emission category among peatland, inundated and mineral land emissions. There is high year-to-year variability in the fluxes. Connecting the year-to-year variability to environmental drivers remains as a future task, as well as studying whether the time series contain any significant trends.

This project has received funding from the European Union’s Horizon Europe research and innovation programme under grant agreement No 101081395

Table 4.1.1: *Methane emission components for European domain from JSBACH-HIMMELI in Tg(CH_4)/yr for an area of 35°N to 73°N and 12.1°W to 37.8°E. Mineral soil flux is the total of dry soil uptake and wet soil emission.*

Year	Peatland emission Tg(CH_4)/yr	Inundated soil Tg(CH_4)/yr	Mineral soil flux Tg(CH_4)/yr	Total Tg(CH_4)/yr
2000	3.55	1.28	-0.85	3.39
2001	3.40	1.22	-0.80	3.21
2002	3.74	1.22	-0.91	3.54
2003	3.83	1.17	-0.97	3.63
2004	3.51	1.24	-0.91	3.34
2005	3.63	1.15	-0.94	3.39
2006	3.63	1.16	-0.94	3.38
2007	3.49	1.21	-0.95	3.23
2008	3.28	1.20	-0.90	3.03
2009	3.53	1.22	-0.90	3.34
2010	3.55	1.36	-0.84	3.54
2011	3.78	1.21	-0.91	3.54
2012	3.34	1.27	-0.84	3.20
2013	3.94	1.22	-0.91	3.74
2014	3.89	1.23	-0.92	3.63
2015	3.45	1.20	-1.01	3.18
2016	3.66	1.27	-0.92	3.47
2017	3.47	1.24	-0.88	3.27
2018	3.87	1.26	-0.97	3.70
2019	3.42	1.42	-0.98	3.37
2020	3.82	1.56	-0.96	3.87
2021	3.63	1.29	-0.97	3.47
2022	3.70	1.25	-1.02	3.47

This project has received funding from the European Union's Horizon Europe research and innovation programme under grant agreement No 101081395

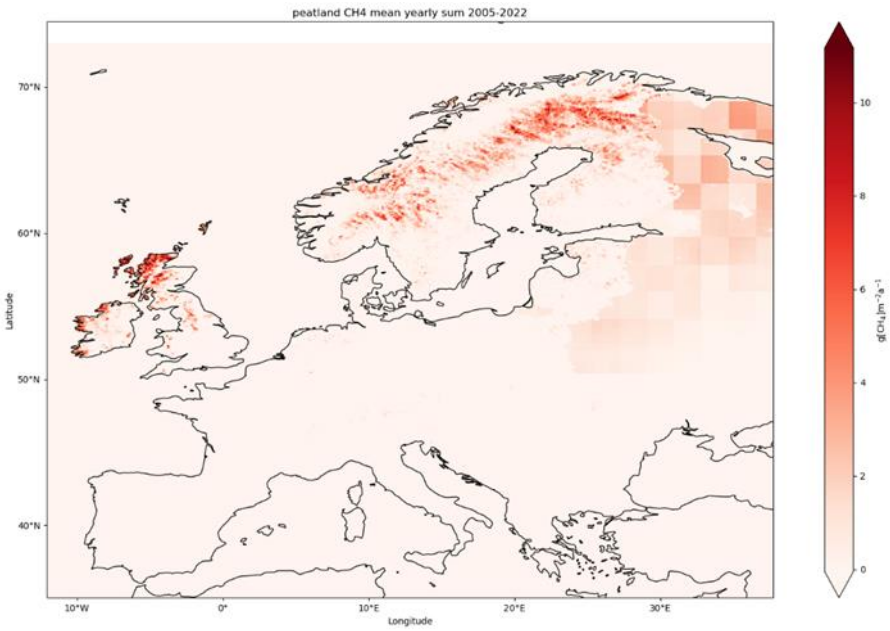

Figure 4.1.1: *Peatland emissions from JSBACH-HIMMELI within the area of EYE-CLIMA European domain. Average over years 2000 – 2022.*

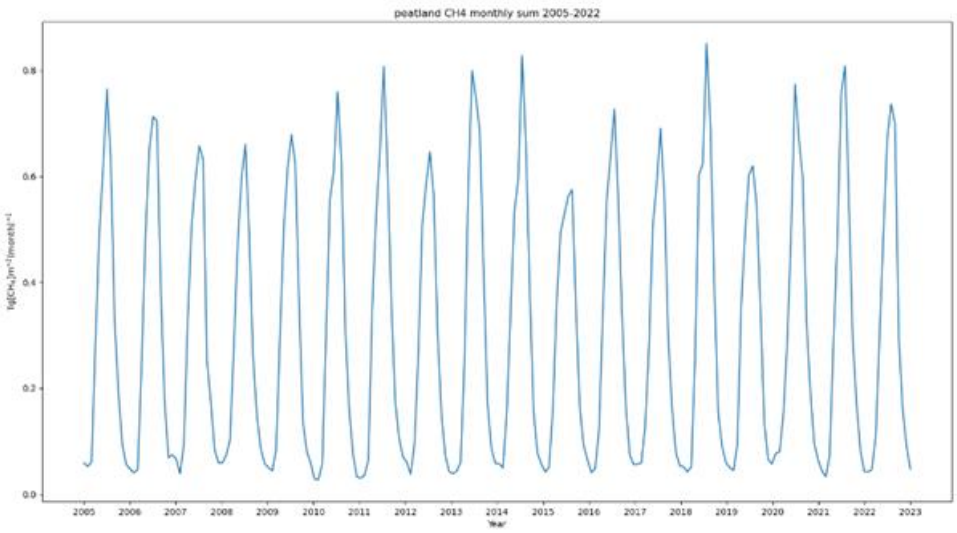

Figure 4.1.2: *Monthly European peatland fluxes from JSBACH-HIMMELI for years 2000 - 2022 in Tg (CH_4)/month.*

This project has received funding from the European Union's Horizon Europe research and innovation programme under grant agreement No 101081395

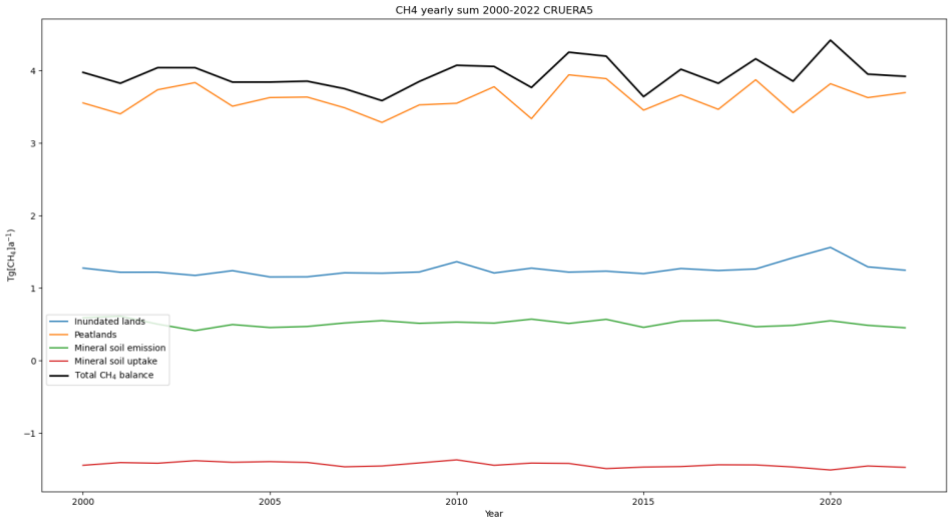

Figure 4.1.3: *Annual total European methane flux components from JSBACH-HIMMELI for years 2000 - 2022 in Tg (CH_4)/month.*

Inundated soils

Inundated areas are located at the low-lying land near lakes, rivers and coastlines. The mean European inundated soil methane fluxes reflect this distribution (Figure 4.1.4) and the variations in fluxes are driven by the heterotrophic soil respiration rate. The inundated soil distribution is dynamic and has high year-to-year and seasonal variation due to precipitation changes and due to snow melt causing spring flooding. This is reflected in monthly inundated soil methane emissions (Figure 4.1.5) as well as in the annual emissions (Table 4.1.1 and Figure 4.1.3). Year 2020 had anomalously high inundated soil methane emissions. Inundated land emissions are a significant contributor to the European terrestrial methane budget, and their temporal variability underlines their importance to be included in the inversion priors.

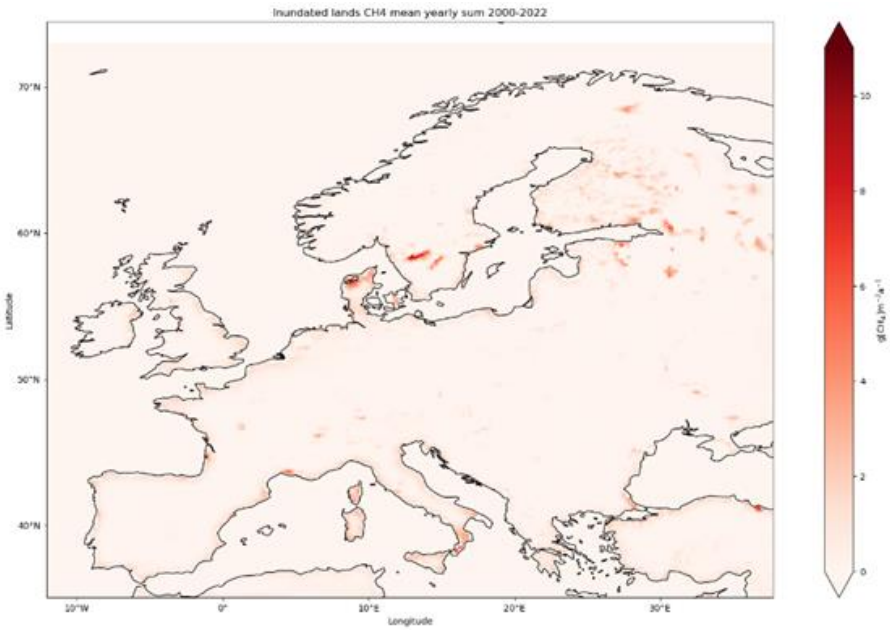

Figure 4.1.4: *Inundated land emissions from JSBACH-HIMMELI within the area of EYE-CLIMA European domain. Average over years 2000 – 2022.*

This project has received funding from the European Union's Horizon Europe research and innovation programme under grant agreement No 101081395

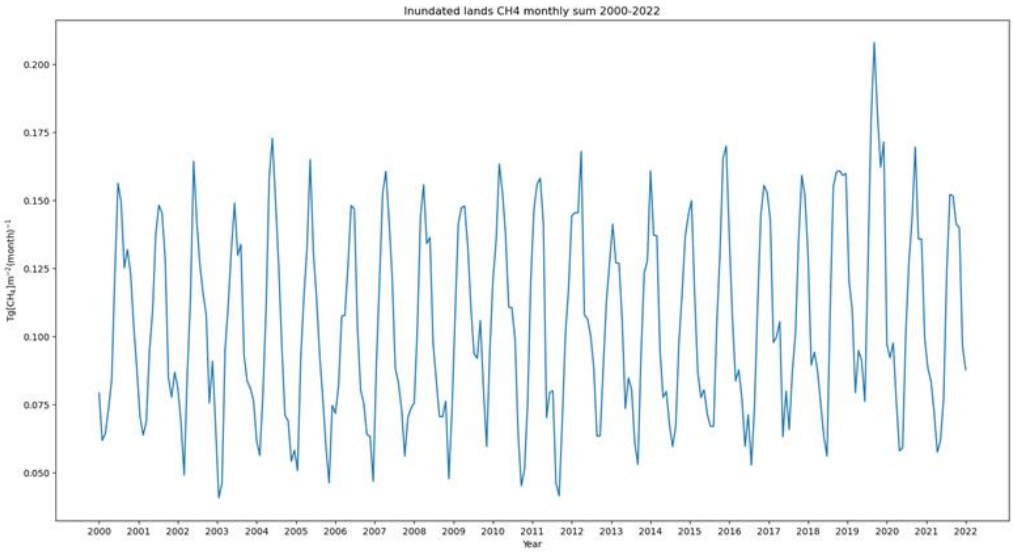

Figure 4.1.5: *Monthly European inundated land fluxes from JSBACH-HIMMELI for years 2000 - 2022 in Tg (CH_4)/month.*

Mineral soils

Mineral soil emissions include both dry mineral soil uptake and wet mineral soil emissions. These components are added together and the annual average mineral soil fluxes are given in Table 4.1.1. The average fluxes suggest methane uptake by mineral soils every year. The map over Europe (Figure 4.1.6) shows that the emissions occur in regions with high precipitation, along coastlines and mountainous regions. Winter periods in the UK and Ireland have especially high emissions. The time series of the dry mineral soil and wet mineral soil flux components are presented in Fig 4.1.3, which shows that their year-to-year variability is modest, and the flux magnitudes are smaller than peatland emissions, but they still contribute by a significant amount to the total budget. The month-to-month variability of the fluxes (Figure 4.1.7) is quite large due to soil moisture changes from winter to summer seasons and due to precipitation changes. Total methane emissions including all components are shown in Figure 4.1.8.

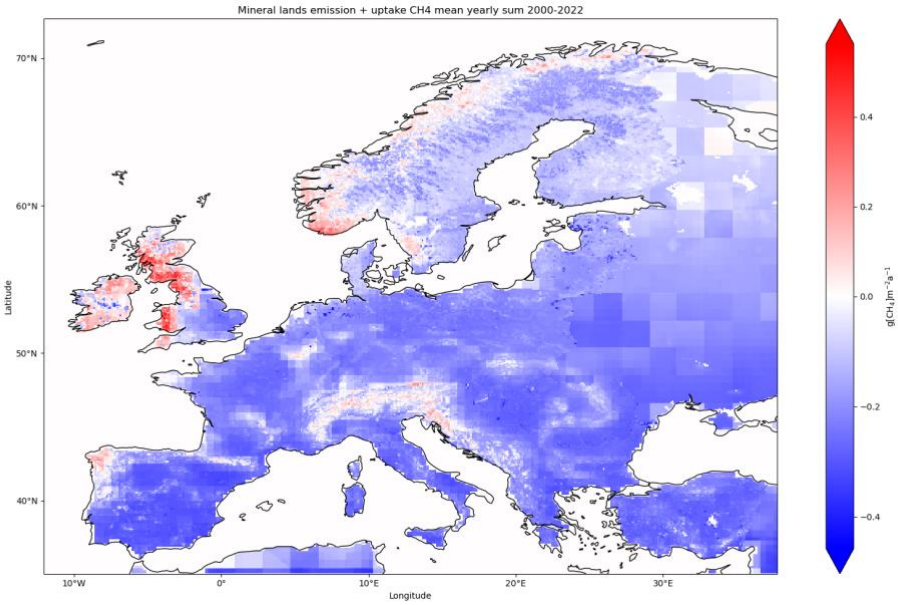

Figure 4.1.6: *Mineral soil fluxes from JSBACH-HIMMELI within the area of EYE-CLIMA European domain. Average over years 2000 – 2022.*

This project has received funding from the European Union's Horizon Europe research and innovation programme under grant agreement No 101081395

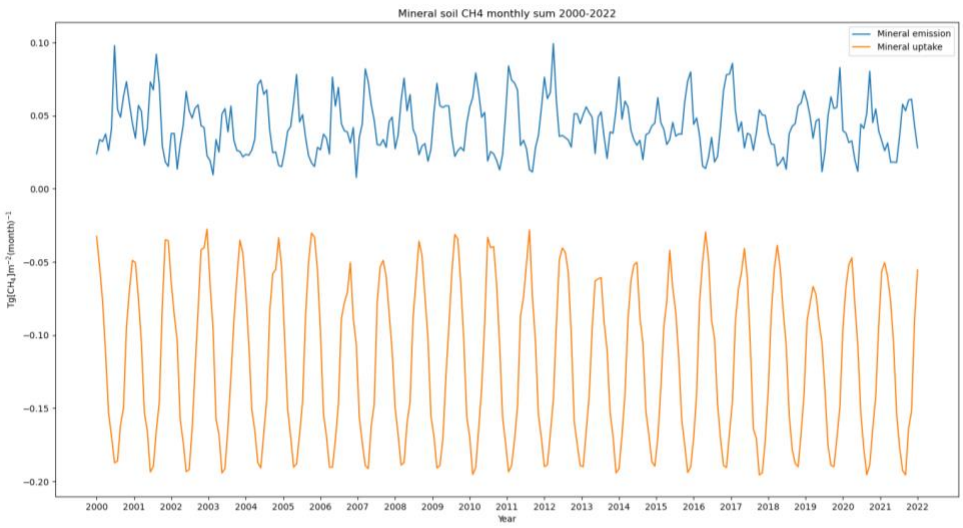

***Figure 4.1.7**: Monthly European mineral soil fluxes from JSBACH-HIMMELI for years 2000 - 2022 in Tg (CH_4)/month.*

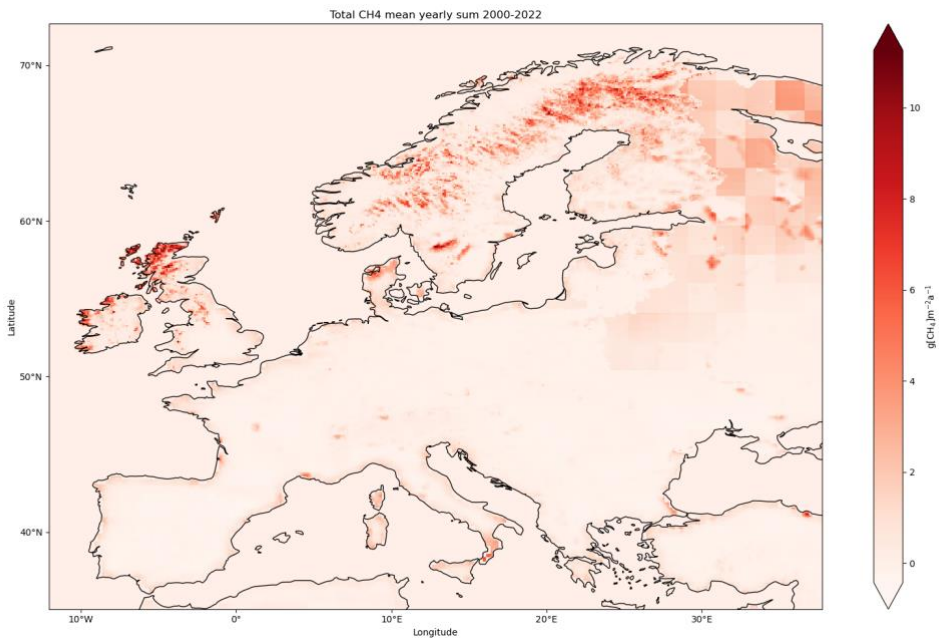

***Figure 4.1.8:** Total biospheric methane fluxes from JSBACH-HIMMELI within the area of EYE-CLIMA European domain. Average over years 2000 – 2022.*

4.2 ORCHIDEE

Model description for the CH_4 fluxes

A different version of ORCHIDEE than the one used for CO_2 and N_2O fluxes has been employed for this first round of simulations. It is based on the ORCHIDEE-PEAT version, described in Salmon et al. (2022). ORCHIDEE-PEAT integrates the peatland soil hydrology to simulate waterlogged conditions, process-based module for soil temperature that simulates soil freezing, thawing and phase change-induced heat fluxes in the soil, a photosynthesis scheme of a mixed plant species northern peatland ecosystem and a scheme of peat accumulation and decomposition to CO_2 for three soil carbon pools: active, slow and passive, which are vertically discretized (Qiu et al., 2019). The methane scheme includes:

This project has received funding from the European Union's Horizon Europe research and innovation programme under grant agreement No 101081395

1) methanogenesis of the three carbon pools, 2) methane and oxygen transport in the soil and snow layers, 3) transport of methane to the atmosphere by ebullition, 4) plant mediated transport and 5) methanotrophy by soil oxic conditions and roots exudates. The model was calibrated and evaluated on 14 northern peatland sites distributed on both the Eurasian and American continents in the northern boreal and temperate regions. Data assimilation approaches were employed to optimise parameters at all sites simultaneously. The model simulates methane emissions from peatlands and inundated soils. CH4 fluxes simulated with the Salmon et al (2022) model version are presented below.

Unfortunately, the coupling of these methane-specific developments into the trunk version of ORCHIDEE, to have a comprehensive set of fluxes (including CO_2, CH_4 and N_2O) is still under completion, due to unforeseen complex technical difficulties. In addition, we could not easily re-run the initial ORCHIDEE-PEAT version with the new high resolution climate forcing, given some changes in the overall code management software, linked to the need of running in parallel mode at high resolution. In this context, we thus briefly provide below a simple analysis of the initial ORCHIDEE-PEAT model simulation, that was done at a coarser resolution (at 1°). These fluxes only cover the period 2004 to 2014 and will thus only potentially be used as a climatology for the atmospheric inversion and the overall CH_4 synthesis. However, a simulation at high resolution with the selected forcing (ERA5land + CRU) should be available at the end of the summer 2024 with this model version and could thus be used as a test for the prior fluxes (compared to JSBACH-HIMMELI).

Flux estimates

Figure 4.2.1 and Table 4.2.1 provide an illustration of the spatial and temporal distribution of the simulated CH_4 emissions with the ORCHIDEE-PEAT model version at coarse resolution and only over the period 2004 - 2014. Like with JSBACH-HIMMELI, the maximum CH4 emissions are located in northern Europe and to a lower extent northern United Kingdom. The differences in spatial resolution between the two model simulations prevent a much more meaningful comparison of the spatial distribution. With respect to the temporal evolution, Figure 4.2.1 shows high emission in 2004, 2008 and 2012 for ORCHIDEE-PEAT. These maximums do not correspond to maximum emissions with JSBACH-HIMMELI, likely due to different wetland extent dynamics and climate forcing. We will investigate more deeply the driver of the model differences, once the simulation at high resolution with ORCHIDEE-PEAT will be performed.

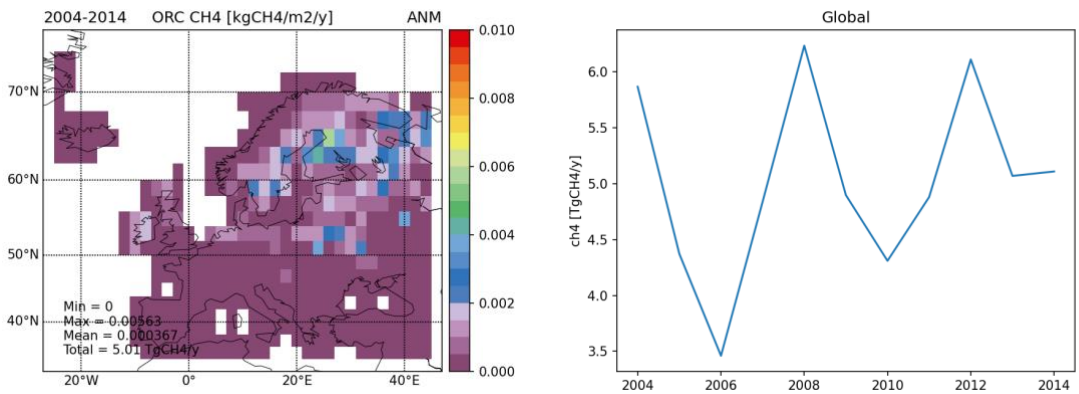

Figure 4.2.1: *Left: Map of the annual methane emission from peatland from ORCHIDEE in kgCH$_4$/m^2/yr. Right: temporal evolution of these methane emission for an area of 35°N to 73°N and 12.1°W to 37.8°E.*

This project has received funding from the European Union's Horizon Europe research and innovation programme under grant agreement No 101081395

Table 4.2.1: *Methane emission components for the European domain from ORCHIDEE in Tg(CH_4)/yr for an area of 35°N to 73°N and 12.1°W to 37.8°E. Only the total Peatland plus inundated soil emission is provided in this first version.*

Year	Peatland emission + inundated soil Tg(CH_4)/yr
2004	5.87
2005	4.37
2006	3.46
2007	4.84
2008	6.24
2009	4.90
2010	4.31
2011	4.88
2012	6.11
2013	5.07
2014	5.11

4.3 Uncertainties

Wetlands

The European terrestrial methane emissions contain many uncertainties related to climate drivers, land cover, inundated area, peatland process model parameters and model structures, mineral soil parameterizations etc.

For land cover the uncertainties are related to plant functional type distributions and soil type descriptions affecting the soil moisture and water table conditions in the soil as well as amount of substrate for methane production. Inundated area, when using a prescribed satellite-product, has uncertainties due to possible overlap with lakes and other water bodies, and forests obstructing the view to inundated surface. Mineral soil emissions are very uncertain due to limited information on moisture threshold for methane emission, and challenges with soil moisture simulations.

Peatland process parameters have been optimized previously for individual sites (e.g., Susiluoto et al., 2018), and those optimised parameter value distributions need to be taken into use in regional simulations for estimating the European scale flux uncertainties. Uncertainties due to model structures can be taken into account by considering more than one model.

Using different climate drivers may cause significant differences in European methane budgets, and thus more than one driver dataset should be used for sensitivity analysis. The driver datasets may have differences in daily / monthly aggregated values as well as in long term trends. Examples of impact of two driver datasets (CERRA, CRU-ERA) are shown in Figure 4.3.1 for grid-cell simulated surface soil moisture, water table, GPP and methane.

This project has received funding from the European Union's Horizon Europe research and innovation programme under grant agreement No 101081395

In future, studies need to be continued of the role of the different components in the total uncertainty, and guidelines need to be prepared for estimation of the regional simulation uncertainties in order to consistently use them in atmospheric inversions together with the other prior uncertainty sources.

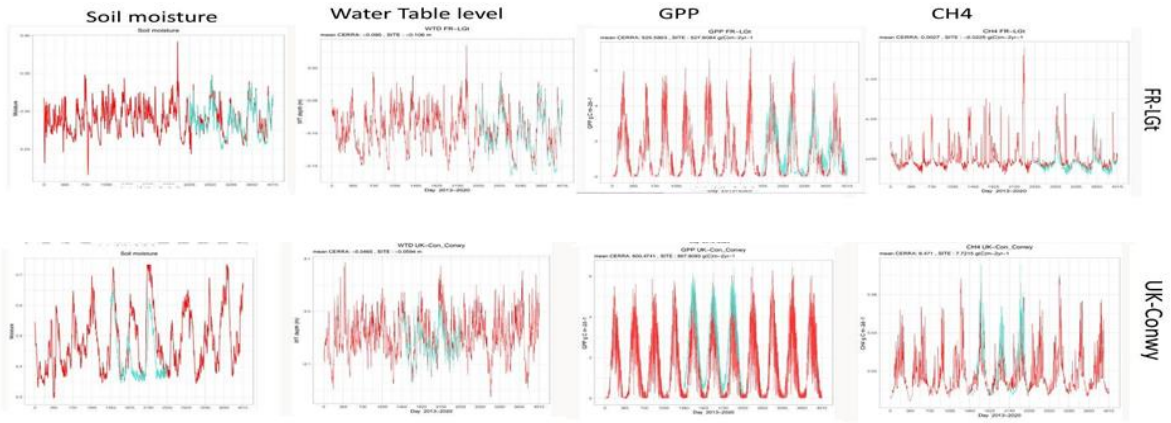

Figure 4.3.1: *Surface soil moisture, water table level, GPP and methane fluxes simulated in two European wetland sites with JSBACH-HIMMELI, using either CERRA (red) or CRU-ERA (blue) climate data as input.*

5. Conclusions

Carbon dioxide, methane and nitrous oxide balances of terrestrial ecosystems have been produced using three process-based models (ORCHIDEE, LPJ-GUESS and JSBACH-HIMMELI, using two models for each species). The carbon dioxide flux products cover Europe over years 1951-2022, nitrous oxide results over years 1901 – 2022 and methane balance products for years 2000-2022. The flux estimates will be used as prior data in the atmospheric inversion modelling task in WP3 and for synthesis of national GHG budgets in WP4. The applied aerial domains as well as time coverages and resolutions may limit the applicability of the products. Significant differences are obtained between the selected models for each species. A more in-depth analysis of the causes of these differences are under investigation and will be reported in the next deliverable. Note also that these simulated fluxes correspond to the first round of model simulations; an updated version will be delivered in the version of this deliverable.

This project has received funding from the European Union's Horizon Europe research and innovation programme under grant agreement No 101081395

6. References

Cleveland, C. C., Townsend, A. R., Schimel, D. S., Fisher, H., Howarth, R. W., Hedin, L. O., ... & Wasson, M. F. (1999). Global patterns of terrestrial biological nitrogen (N2) fixation in natural ecosystems. *Global biogeochemical cycles*, *13*(2), 623-645.

Curry, C. L. (2007). Modeling the soil consumption of atmospheric methane at the global scale, Global Biogeochem. Cycles., 21, GB4012-1-15, doi:10.1029/2006GB002818

De Rosnay, P., Polcher, J. D., Bruen, M., & Laval, K. (2002). Impact of a physically based soil water flow and soil-plant interaction representation for modeling large-scale land surface processes. *Journal of Geophysical Research: Atmospheres*, *107*(D11), ACL-3.

D'Orgeval, T., Polcher, J., & De Rosnay, P. (2008). Sensitivity of the West African hydrological cycle in ORCHIDEE to infiltration processes. *Hydrology and Earth System Sciences*, *12*(6), 1387-1401.

Ducoudré, N. I., Laval, K., & Perrier, A. (1993). SECHIBA, a New Set of Parameterizations of the Hydrologic Exchanges at the Land-Atmosphere Interface within the LMD Atmospheric General Circulation Model. *Journal of Climate*, *6*(2), 248–273. https://doi.org/10.1175/1520-0442(1993)006<0248:SANSOP>2.0.CO;2

Reick, C., et al. (2013). Representation of natural and anthropogenic land cover change in MPI-ESM. Journal of Advances in Modeling Earth Systems, 5, 459-482 , https://doi.org/10.1002/jame.20022, 2013.

Raivonen, M., et al. (2017). HIMMELI v1.0: HelsinkI Model of MEthane buiLd-up and emIssion for peatlands. Geoscientific Model Development 10, 4665–4691. https://doi.org/10.5194/gmd-10-4665-2017

Spahni, R., et al. (2011). Constraining global methane emissions and uptake by ecosystems. Biogeosciences 8, 1643–1665. https://doi.org/10.5194/bg-8-1643-2011

Zhang, Z., et al. (2021). Development of the global dataset of Wetland Area and Dynamics for Methane Modeling (WAD2M). Earth System Science Data 13, 2001–2023. https://doi.org/10.5194/essd-13-2001-2021

Batjes, N. H. (2016). Harmonized soil property values for broad-scale modelling (WISE30sec) with estimates of global soil carbon stocks. Geoderma, 269, 61–68. https://doi.org/10.1016/j.geoderma.2016.01.034

Blanc-Betes, E., Kantola, I. B., Gomez-Casanovas, N., Hartman, M. D., Parton, W. J., Lewis, A. L., et al. (2021). In silico assessment of the potential of basalt amendments to reduce N2O emissions from bioenergy crops. GCB Bioenergy, 13(1), 224–241. https://doi.org/10.1111/gcbb.12757

Collatz, G. J., Ribas-Carbo, M., & Berry, J. A. (1992). Coupled photosynthesis-stomatal conductance model for leaves of C4 plants. *Functional Plant Biology*, *19*(5), 519-538.

Farquhar, G. D., von Caemmerer, S. V., & Berry, J. A. (1980). A biochemical model of photosynthetic CO 2 assimilation in leaves of C 3 species. *planta*, *149*, 78-90.

Friedlingstein, P., Jones, M. W., O'Sullivan, M., Andrew, R. M., Bakker, D. C. E., Hauck, J., Le Quéré, C., Peters, G. P., Peters, W., Pongratz, J., Sitch, S., Canadell, J. G., Ciais, P., Jackson, R. B., Alin, S. R., Anthoni, P., Bates, N. R., Becker, M., Bellouin, N., … Zeng, J. (2022). Global Carbon Budget 2021. *Earth System Science Data*, *14*(4), 1917–2005. https://doi.org/10.5194/essd-14-1917-2022

Krinner, G., Viovy, N., de Noblet-Ducoudré, N., Ogée, J., Polcher, J., Friedlingstein, P., Ciais, P., Sitch, S., & Prentice, I. C. (2005). A dynamic global vegetation model for studies of the coupled atmosphere-

This project has received funding from the European Union's Horizon Europe research and innovation programme under grant agreement No 101081395

biosphere system: DVGM FOR COUPLED CLIMATE STUDIES. *Global Biogeochemical Cycles*, *19*(1). https://doi.org/10.1029/2003GB002199

Li, C., Aber, J., Stange, F., Butterbach-Bahl, K., and Papen, H.: A process-oriented model of N2O and NO emissions from forest soils: 1. Model development, J. Geophys. Res.-Atmos., 105, 4369–4384, https://doi.org/10.1029/1999JD900949, 2000.

Lindeskog, M., Arneth, A., Bondeau, A., Waha, K., Seaquist, J., Olin, S., & Smith, B. (2013). Implications of accounting for land use in simulations of ecosystem carbon cycling in Africa. Earth System Dynamics, 4(2), 385–407. https://doi.org/10.5194/esd-4-385-2013

Lindeskog, M., Smith, B., Lagergren, F., Sycheva, E., Ficko, A., Pretzsch, H., & Rammig, A. (2021). Accounting for forest management in the estimation of forest carbon balance using the dynamic vegetation model LPJ-GUESS (v4.0, r9710): Implementation and evaluation of simulations for Europe. Geoscientific Model Development (Vol. 14). https://doi.org/10.5194/gmd-14-6071-2021

Liu, B., Mørkved, P. T., Frostegård, Å., & Bakken, L. R. (2010). Denitrification gene pools, transcription and kinetics of NO, N2O and N2 production as affected by soil pH. FEMS Microbiology Ecology, 72(3), 407–417. https://doi.org/10.1111/j.1574-6941.2010.00856.x

Lurton, T., Balkanski, Y., Bastrikov, V., Bekki, S., Bopp, L., Braconnot, P., ... & Boucher, O. (2020). Implementation of the CMIP6 Forcing Data in the IPSL-CM6A-LR Model. *Journal of Advances in Modeling Earth Systems*, *12*(4), e2019MS001940.

Ma, J., Rabin, S. S., Anthoni, P., Bayer, A. D., Nyawira, S. S., Olin, S., et al. (2022b). Assessing the impacts of agricultural managements on soil carbon stocks, nitrogen loss and crop production - a modelling study in eastern Africa. Biogeosciences, 19(8), 2145–2169. https://doi.org/10.5194/bg-19-2145-2022

Ma, J., Olin, S., Anthoni, P., Rabin, S. S., Bayer, A. D., Nyawira, S. S., & Arneth, A. (2022a). Modeling symbiotic biological nitrogen fixation in grain legumes globally with LPJ-GUESS (v4.0 , r10285). Geoscientific Model Development, 15(2), 815–839. https://doi.org/10.5194/gmd-15-815-2022

Maag, M., & Vinther, F. P. (1996). Nitrous oxide emission by nitrification and denitrification in different soil types and at different soil moisture contents and temperatures. Applied Soil Ecology, 4, 5–14.

Meinshausen, M., Nicholls, Z. R. J., Lewis, J., Gidden, M. J., Vogel, E., Freund, M., et al. (2020). The shared socio-economic pathway (SSP) greenhouse gas concentrations and their extensions to 2500. Geoscientific Model Development, 13(8), 3571–3605. https://doi.org/10.5194/gmd-13-3571-2020

Olin, S., Schurgers, G., Lindeskog, M., Wårlind, D., Smith, B., Bodin, P., et al. (2015). Modelling the response of yields and tissue C : N to changes in atmospheric CO2 and N management in the main wheat regions of western Europe. Biogeosciences, 12(8), 2489–2515. https://doi.org/10.5194/bg-12-2489-2015

Parton, W. J., Scurlock, J. M. O., Ojima, D. S., Gilmanov, T. G., Scholes, R. J., Schimel, D. S., et al. (1993). Observations and modeling of biomass and soil organic matter dynamics for the grassland biome worldwide. Global Biogeochemical Cycles, 7(4), 785–809. https://doi.org/10.1029/93GB02042

Portmann, F. T., Siebert, S., & Döll, P. (2010). MIRCA2000-Global monthly irrigated and rainfed crop areas around the year 2000: A new high-resolution data set for agricultural and hydrological modeling. Global Biogeochemical Cycles, 24(1), 1–24. https://doi.org/10.1029/2008gb003435

Prentice, I. C., Cramer, W., Harrison, S. P., Leemans, R., Monserud, R. A., & Solomon, A. M. (1992). Special paper: a global biome model based on plant physiology and dominance, soil properties and climate. *Journal of biogeography*, 117-134.

This project has received funding from the European Union's Horizon Europe research and innovation programme under grant agreement No 101081395

Raoult, N., Edouard-Rambaut, L. A., Vuichard, N., Bastrikov, V., Lansø, A. S., Guenet, B., & Peylin, P. (2024). Using Free Air CO 2 Enrichment data to constrain land surface model projections of the terrestrial carbon cycle. *Biogeosciences*, *21*(4), 1017-1036.

Rochester, I. J. (2003). Estimating nitrous oxide emissions from flood-irrigated alkaline grey clays. Australian Journal of Soil Research, 41(2), 197–206. https://doi.org/10.1071/SR02068

Smith, B., Wårlind, D., Arneth, A., Hickler, T., Leadley, P., Siltberg, J., & Zaehle, S. (2014). Implications of incorporating N cycling and N limitations on primary production in an individual-based dynamic vegetation model. Biogeosciences, 11(7), 2027–2054. https://doi.org/10.5194/bg-11-2027-2014

Susiluoto, J., Raivonen, M., Backman, L., Laine, M., Makela, J., Peltola, O., Vesala, T., Aalto, T., 2018. Calibrating the sqHIMMELI v1.0 wetland methane emission model with hierarchical modeling and adaptive MCMC. Geoscientific Model Development 11, 1199–1228. https://doi.org/10.5194/gmd-11-1199-2018

Tian, H., Yang, J., Lu, C., Xu, R., Canadell, J. G., Jackson, R. B., et al. (2018). The global N2O model intercomparison project. Bulletin of the American Meteorological Society, 99(6), 1231–1251. https://doi.org/10.1175/BAMS-D-17-0212.1

Tian, H., Bian, Z., Shi, H., Qin, X., Pan, N., Lu, C., et al. (2022). History of anthropogenic Nitrogen inputs (HaNi) to the terrestrial biosphere: a 5 arcmin resolution annual dataset from 1860 to 2019. Earth System Science Data, 14(10), 4551–4568. https://doi.org/10.5194/essd-14-4551-2022

Val Martin, M., Blanc-Betes, E., Ming Fung, K., Kantzas, E. P., Kantola, I. B., Chiaravalloti, I., et al. (2023). Improving nitrogen cycling in a land surface model (CLM5) to quantify soil N2O, NO and NH3 emissions from enhanced rock weathering with croplands. Geosci. Model Dev., (16), 5783–5801. https://doi.org/10.5194/gmd-16-5783-2023

Vuichard, N., Messina, P., Luyssaert, S., Guenet, B., Zaehle, S., Ghattas, J., ... & Peylin, P. (2019). Accounting for carbon and nitrogen interactions in the global terrestrial ecosystem model ORCHIDEE (trunk version, rev 4999): Multi-scale evaluation of gross primary production. *Geoscientific Model Development*, *12*(11), 4751-4779.

Wagena, M. B., Bock, E. M., Sommerlot, A. R., Fuka, D. R., & Easton, Z. M. (2017). Development of a nitrous oxide routine for the SWAT model to assess greenhouse gas emissions from agroecosystems. Environmental Modelling and Software, 89, 131–143. https://doi.org/10.1016/j.envsoft.2016.11.013

Waha, K., Van Bussel, L. G. J., Müller, C., & Bondeau, A. (2012). Climate-driven simulation of global crop sowing dates. Global Ecology and Biogeography, 21(2), 247–259. https://doi.org/10.1111/j.1466-8238.2011.00678.x

Wang, T., Ottlé, C., Boone, A., Ciais, P., Brun, E., Morin, S., ... & Peng, S. (2013). Evaluation of an improved intermediate complexity snow scheme in the ORCHIDEE land surface model. *Journal of Geophysical Research: Atmospheres*, *118*(12), 6064-6079.

Wang, F., Cheruy, F., & Dufresne, J. L. (2016). The improvement of soil thermodynamics and its effects on land surface meteorology in the IPSL climate model. *Geoscientific Model Development*, *9*(1), 363-381.

Wårlind, D., Smith, B., Hickler, T., & Arneth, A. (2014). Nitrogen feedbacks increase future terrestrial ecosystem carbon uptake in an individual-based dynamic vegetation model. Biogeosciences, 11(21), 6131–6146. https://doi.org/10.5194/bg-11-6131-2014

Weier, K. L., Doran, J. W., Power, J. F., & Walters, D. T. (1993). Denitrification and the Dinitrogen/Nitrous Oxide Ratio as Affected by Soil Water, Available Carbon, and Nitrate. Soil Science Society of America Journal, 57(1), 66–72. https://doi.org/10.2136/sssaj1993.03615995005700010013x

This project has received funding from the European Union's Horizon Europe research and innovation programme under grant agreement No 101081395

Winkler, K., Fuchs, R., Rounsevell, M., & Herold, M. (2021). Global land use changes are four times greater than previously estimated. Nature Communications, 12, 2501. https://doi.org/10.1038/s41467-021-22702-2

Xu-Ri, & Prentice, I. C. (2008). Terrestrial nitrogen cycle simulation with a dynamic global vegetation model. Global Change Biology, 14(8), 1745–1764. https://doi.org/10.1111/j.1365-2486.2008.01625.x

Yin, X., & Struik, P. C. (2009). C3 and C4 photosynthesis models: An overview from the perspective of crop modelling. *NJAS-Wageningen Journal of Life Sciences*, *57*(1), 27-38.

Zaehle, S., & Friend, A. D. (2010). Carbon and nitrogen cycle dynamics in the O-CN land surface model: 1. Model description, site-scale evaluation, and sensitivity to parameter estimates. Global Biogeochemical Cycles, 24(1), 1–13. https://doi.org/10.1029/2009GB003521

Zhang, B., Zhou, M., Zhu, B., Kemmann, B., Pfülb, L., Burkart, S., et al. (2023). Threshold-like effect of soil NO3− concentrations on denitrification product N2O/(N2O+N2) ratio is mediated by soil pH. Soil Biology and Biochemistry, 187, 109213. https://doi.org/10.1016/j.soilbio.2023.109213

This project has received funding from the European Union's Horizon Europe research and innovation programme under grant agreement No 101081395

https://eyeclima.eu

BRUSSELS, 28 06 2024

Funded by the European Union. Views and opinions expressed are however those of the author(s) only and do not necessarily reflect those of the European Union. Neither the European Union nor the granting authority can be held responsible for them.

This project has received funding from the European Union's Horizon Europe research and innovation programme under grant agreement No 101081395